



HAL
open science

Intrabacterial lipid inclusions in mycobacteria: unexpected key players in survival and pathogenesis?

Ivy Mallick, Pierre Santucci, Isabelle Poncin, Vanessa Point, Laurent Kremer,
Jean-François Cavalier, Stéphane Canaan

► **To cite this version:**

Ivy Mallick, Pierre Santucci, Isabelle Poncin, Vanessa Point, Laurent Kremer, et al.. Intrabacterial lipid inclusions in mycobacteria: unexpected key players in survival and pathogenesis?. FEMS Microbiology Reviews, 2021, 10.1093/femsre/fuab029 . hal-03255780

HAL Id: hal-03255780

<https://amu.hal.science/hal-03255780>

Submitted on 9 Jun 2021

HAL is a multi-disciplinary open access archive for the deposit and dissemination of scientific research documents, whether they are published or not. The documents may come from teaching and research institutions in France or abroad, or from public or private research centers.

L'archive ouverte pluridisciplinaire **HAL**, est destinée au dépôt et à la diffusion de documents scientifiques de niveau recherche, publiés ou non, émanant des établissements d'enseignement et de recherche français ou étrangers, des laboratoires publics ou privés.

Intrabacterial lipid inclusions in mycobacteria: unexpected key players in survival and pathogenesis?

Ivy Mallick^{1,2*}, Pierre Santucci^{1##}, Isabelle Poncin¹, Vanessa Point¹, Laurent Kremer^{3,4},
Jean-François Cavalier¹ and Stéphane Canaan^{1§}

¹ Aix-Marseille Univ, CNRS, LISM, IMM FR3479, Marseille, France

² IHU Méditerranée Infection, Aix-Marseille Univ., Marseille, France

³ Institut de Recherche en Infectiologie de Montpellier (IRIM), CNRS, UMR 9004, Université de Montpellier, Montpellier, France.

⁴ IRIM, INSERM, Montpellier, France.

Present address: Host Pathogen Interactions in Tuberculosis Laboratory, The Francis Crick Institute, London NW1 1AT, England, United Kingdom

* Both authors contributed equally to this work, and should be considered as first co-authors.

§ Correspondence address to Stéphane Canaan, canaan@imm.cnrs.fr.

Short title: ILI in mycobacterial lifecycle

Keywords: Metabolic adaptation, mycobacterial lipids, persistence, triacylglycerol, tuberculosis.

Abbreviations:

Acylglycerol-3-phosphate acyltransferase (AGPAT); bone marrow-derived macrophage (BMDM); diacylglycerol (DAG); diacylglycerol-acyltransferase (DGAT); dormancy survival regulator (Dos); fatty acid transport proteins (FATP); foamy macrophage (FM); free fatty acid (FFA); glycerol-3-phosphate (G3P); glycerol-3-phosphate acyltransferase (GPAT); heparin-binding hemagglutinin adhesin (HBHA); intrabacterial lipid inclusion/Intracytosolic lipid inclusion (ILI); latent TB infection (LTBI); lipid droplet (LD); lysophosphatidic acid (LPA); monoacylglycerol (MAG); *Mycobacterium abscessus* (*Mabs*); *Mycobacterium avium* (*Mav*); *Mycobacterium bovis* BCG (*Mbv* BCG); *Mycobacterium marinum* (*Mmar*); *Mycobacterium smegmatis* (*Msmeg*); *Mycobacterium tuberculosis* (*Mtb*); nitric oxide (NO); non-tuberculous mycobacteria (NTM); oleic acid (OA); peripheral blood mononuclear cells (PBMCs); phosphatidic acid (PA); phosphatidic acid phosphatase (PAP); tetrahydrolipstatin (THL); thin layer chromatography (TLC); triacylglycerol (TAG); triacylglycerol synthase

33 (TGS); tricarboxylic acid cycle (TCA);tuberculosis (TB); very low density lipoprotein (VLDL);
34 wax ester (WE); wild-type (WT).

35 **Abstract:**

36 Mycobacterial species, including *Mycobacterium tuberculosis*, rely on lipids to survive and
37 chronically persist within their hosts. Upon infection, opportunistic and strict pathogenic
38 mycobacteria exploit metabolic pathways to import and process host-derived free fatty
39 acids, subsequently stored as triacylglycerols under the form of intrabacterial lipid inclusions
40 (ILI). Under nutrient-limiting conditions, ILI constitute a critical source of energy that fuels
41 the carbon requirements and maintain redox homeostasis, promoting bacterial survival for
42 extensive periods of time. In addition to their basic metabolic functions, these organelles
43 display multiple other biological properties, emphasizing their central role in the
44 mycobacterial lifecycle. However, despite of their importance, the dynamics of ILI
45 metabolism and their contribution to mycobacterial adaptation/survival in the context of
46 infection has not been thoroughly documented. Herein, we provide an overview of the
47 historical ILI discoveries, their characterization, and current knowledge regarding the micro-
48 environmental stimuli conveying ILI formation, storage and degradation. We also review
49 new biological systems to monitor the dynamics of ILI metabolism in extra- and intracellular
50 mycobacteria and describe major molecular actors in triacylglycerol biosynthesis,
51 maintenance and breakdown. Finally, emerging concepts regarding to the role of ILI in
52 mycobacterial survival, persistence, reactivation, antibiotic susceptibility and inter-individual
53 transmission are also discuss.

54

55

56 **Introduction**

57 Tuberculosis (TB), caused by *Mycobacterium tuberculosis* (*Mtb*), remains a global health
58 issue and one of the deadliest disease caused by a single infectious agent (WHO 2020).
59 Upon primary infection by *Mtb*, granulomas constrain the infection by limiting *Mtb* replication
60 and dissemination within the lungs. If for some individuals these dynamic and complex
61 immunological structures may confer a protective effect by clearing the infection, some of
62 them however are not able to fully eradicate the pathogen. Indeed, *Mtb* possesses the
63 remarkable ability to persist within its host for extensive period of time without generating
64 any clinical symptoms, before eventual reactivation that causes the active form of the
65 disease (Ramakrishnan 2012, Russell 2001, Russell 2007). Recent advances have
66 suggested that the current and commonly accepted estimation that 25-30% of the world's
67 population are infected with TB and at risk of developing TB disease might be
68 overestimated highlighting that more evidences are required to better define host clearance
69 and bacterial persistence in the context of TB pathogenesis (Behr, et al. 2019). Therefore,
70 understanding the cellular and molecular bases for *Mtb* clearance, survival, persistence and
71 reactivation within granulomas remains a fundamental challenge, with the ultimate goal of
72 developing new tools and approaches to better control TB.

73 It is now clearly established that host-derived lipids such as triacylglycerols (TAG),
74 cholesterol, phospholipids and free fatty acids (FFA) are being used for *Mtb* survival *in vivo*,
75 by providing energy inside granulomatous lesions, therefore emphasizing the essential role
76 of central lipid metabolism in mycobacterial long-term survival and persistence (Bloch and
77 Segal 1956, Lee, et al. 2013, McKinney, et al. 2000, Nazarova, et al. 2017). During this
78 specific phase, designated latent TB infection (LTBI), *Mtb* may harbour a wide range of
79 phenotypes which is often dependent on the host-local immune state. However, very few
80 bacilli are able to actively replicate and most of them are assumed to be in a slow/non-
81 replicating state. This phenotypic behaviour is characterized by major and systematic
82 physiological features such as low metabolic activity, bacterial division arrest, loss of acid
83 fastness, increased antibiotics tolerance and presence of large amounts of TAG stored
84 under the form of intracytosolic / intrabacterial lipid inclusions (ILI) (Caire-Brandli, et al.
85 2014, Daniel, et al. 2016, Daniel, et al. 2011, Garton, et al. 2002, Garton, et al. 2008,
86 Kapoor, et al. 2013, Santucci, et al. 2019a, Vilcheze and Kremer 2017).

87 TAG are neutral lipids, insoluble in water, comprising of three fatty acids esterified onto a
88 glycerol backbone. They represent prominent energy storage molecules in many living
89 organisms (eukaryotes and prokaryotes) and provide high amounts of ATP when mobilized

90 through the lipolysis and the β -oxidation pathways. Numerous organisms (including some
91 bacteria, parasites, plants and mammals) are able to synthesize TAG and to store them
92 under the form of cytoplasmic granules (Murphy 2001, Murphy 2012). Over the years, these
93 structures have been designated as lipid droplets (LD), lipid bodies, lipid inclusions,
94 adiposomes, fat bodies or oil bodies (Daniel, et al. 2004, Walther and Farese 2009). In a
95 homeostatic view, these organelles have been ascribed to regulate the storage of neutral
96 lipids, remove toxic lipids, involved in cellular communication including stress response
97 mechanisms as well as inflammatory processes (Monson, et al. 2021). In this review, the
98 term LD refers to as the eukaryotic TAG inclusions while ILI designates the bacterial TAG
99 inclusions. With respect to their chemical composition, TAG granules are essentially
100 composed of neutral lipids (*i.e.*, TAG or sterol esters), surrounded by a phospholipid
101 monolayer in which specific proteins, called lipid droplet-associated proteins, are inserted.
102 To date, adipocytes, whose functions are mainly dedicated to the storage of neutral lipids in
103 the form of LD within human body, are probably the best characterized cell type harboring
104 TAG inclusions. In bacteria, species belonging to the *Rhodococcus* and *Mycobacterium*
105 genus have been utilized as model systems to study TAG biosynthesis, ILI formation,
106 storage and hydrolysis (Alvarez 2016, Santucci, et al. 2016, Wältermann and Steinbüchel
107 2005).
108 Nevertheless, with respect to *Mtb*, how the bacilli specifically realign their metabolism *in*
109 *vivo*, use and store host-derived lipids under the form of ILI to persist in a non-replicating
110 state and hydrolyse these lipids during reactivation, still remains poorly understood. The
111 presence of such ILI has also been highlighted in several mycobacterial species including
112 non-tuberculous mycobacteria (NTM), suggesting a conserved function of these lipid
113 structures in the lifestyle of non-pathogenic, opportunistic and strict pathogens (Barisch, et
114 al. 2015, Barisch and Soldati 2017, Santucci, et al. 2019a, Viljoen, et al. 2016) (**Figure 1**).
115 In this review, we summarize the current knowledge and understanding of ILI composition
116 and metabolic actors involved in their formation (synthases) and hydrolysis (lipases) with a
117 special emphasis on mycobacterial species (**Figure 2**). We report how ILI have been
118 discovered and how specific microenvironments govern their biosynthesis/mobilization. A
119 non-exhaustive description of some of the recent approaches developed to study the
120 dynamics of these processes in pathogenic mycobacteria is also presented. These include
121 the development of experimental models, the use of specific classes of pharmacological
122 inhibitors and biochemical and genetic strategies to delineate ILI biology. Finally, the recent

123 discoveries regarding the physiological roles and impacts of these conserved organelles
124 with respect to mycobacterial survival and pathogenicity are discussed.

125

126 ***Historical discovery of TAG storage and intracytoplasmic bacterial lipid inclusions***

127 In prokaryotes, although ILI have been observed in both Gram⁺ and Gram⁻ bacteria, they
128 remain a common characteristic of the *Actinobacteria* phylum (Alvarez and Steinbüchel
129 2002). Indeed, many species belonging to the *Streptomyces*, *Nocardia*, *Dietzia*, *Gordonia*,
130 *Rhodococcus* or *Mycobacterium* genus possess the capacity to synthesize and store TAG
131 in the form of ILI (Alvarez 2016, Alvarez and Steinbüchel 2002). In mycobacterial species,
132 ILI were first observed during the 1940s with the pioneering work of Burdon, Sheenan and
133 Whitwell (Burdon 1946, Sheehan and Whitwell 1949). Using Sudan Black B, a non-
134 fluorescent dye specific for neutral lipids (Hartman 1940), these authors demonstrated the
135 presence of ILI within *in vitro* mycobacterial cultures, in samples isolates from infected
136 guinea pigs, and also within sputum from TB patients (Burdon 1946, Sheehan and Whitwell
137 1949). In the 1950s, the use of electron microscopy enabled, for the first time, imaging
138 single bacterial cell at high-resolution, thereby revealing the presence of globular
139 cytoplasmic structures in *Mycobacterium avium* (*Mav*) as well as in *Mycobacterium leprae*
140 (Brieger and Glauert 1956a, Brieger and Glauert 1956b, Knaysi, et al. 1950). Both studies
141 highlighted the heterogeneity within the population in term of bacterial size, shape and
142 granule content. Interestingly, the authors stated that this type of globules were visible only
143 after long incubation period in a rich culture medium, suggesting a co-relation between
144 bacterial fitness and metabolism with the appearance of the granular structures. The first
145 metabolic studies were carried out later on and demonstrated that supplementation of lipid
146 substrates such as oleic acid (OA) or Tween-80 in the culture medium favoured the
147 appearance of ILI in mycobacterial cells (Schaefer and Lewis 1965). At that time, the exact
148 composition of the accumulated lipids was not established, and there was no mention
149 regarding the exact phase of the bacterial cell cycle wherein these structures were visible
150 (Schaefer and Lewis 1965). In the 1970s, the use of radiolabelled substrates, such as
151 palmitic acid or OA, in *Mav* or *Mycobacterium smegmatis* (*Msmeg*) cultures provided
152 evidence that the FFA incorporated within bacterial cells were mainly stored as TAG rather
153 than simple FFA or phospholipids (Barksdale and Kim 1977, McCarthy 1971, Nakagawa, et
154 al. 1976, Weir, et al. 1972). Using gas chromatography to analyse radiolabelled OA
155 incorporated into TAG, two independent research groups demonstrated that modifications

156 in chain lengths had occurred (Nakagawa, et al. 1976, Weir, et al. 1972). Indeed, most of
157 the stored TAG were composed of labelled C14:0, C16:0, C16:1, C18:1, C20:0 and C24:0
158 long-chain fatty acids, suggesting that the lipid substrates can be either shortened or
159 elongated. Moreover, upon OA treatment, the authors noticed that bacterial TAG
160 accumulation was closely correlated with an increase in triacylglycerol synthase (TGS) (also
161 known as diacylglycerol-acyltransferase; DGAT) activity, and that this phenomenon was
162 exclusively restricted to the post-exponential or stationary growth phases (Nakagawa, et al.
163 1976). Altogether, these early results favoured the emergence of new concepts regarding
164 ILI biosynthesis and led to the assumption that the production of ILI might depend on
165 various factors, in particular the composition of the culture medium as well as the
166 physiological stage of the bacterial cell cycle.

167

168 ***Biophysicochemical factors impacting TAG anabolism and storage in vitro***

169 During their lifecycle, most bacterial species encounter unfavourable environments and are
170 not only facing drastic modifications of surrounding physical and chemical factors but also
171 important fluctuations in nutrient availability. To adapt and survive under such drastic
172 conditions, bacteria have evolved metabolic strategies which include numerous biological
173 pathways and specific molecular factors. In the context of TB, formation of pulmonary
174 granulomatous lesions is one of the major hallmarks of *Mtb* infection. Within granulomas,
175 the bacilli are exposed to various stresses, where the most significant ones are probably
176 nutrient limitation (*i.e.*, carbon, nitrogen, iron starvation etc.), exposure to reactive
177 oxygen/nitrogen intermediates including nitric oxide (NO) and oxygen depletion (Barry, et al.
178 2009, Deb, et al. 2009, Honer zu Bentrup and Russell 2001, Timm, et al. 2003). These
179 harsh conditions, alone or in combination, significantly alter the metabolic state and the
180 fitness of the tubercle bacilli and, consequently, impact on TAG biosynthesis and
181 accumulation (**Figure 3**), which are critical for *Mtb* survival during lung infection and anti-TB
182 chemotherapy (Baek, et al. 2011, Garton, et al. 2008, Hammond, et al. 2015).

183

184 *1) Specificity and bioavailability of carbon source*

185 In infected tissues, several types of lipids derived from both living and dead host cells can
186 be used by the bacilli as a source of carbon and energy to further survive, persist or
187 replicate. Among them, saturated or unsaturated FFA are probably the most abundant
188 lipids, whereas more complex lipids such as phospholipids, glycerides (monoacylglycerol,

189 MAG; diacylglycerol, DAG; TAG or steroids, *i.e.* cholesterol esters derivatives) can be
190 converted into long or short chain FFA and then further imported and reprocessed by the
191 tubercle bacilli (Bloch and Segal 1956, Kim, et al. 2010, Lee, et al. 2013, McKinney, et al.
192 2000, Nazarova, et al. 2017). Interestingly, when cultured in a well-defined medium
193 containing long-chain FFA or dextrose as the sole carbon source, ILI formation monitored
194 by electron microscopy approaches revealed that TAG accumulation was visible only under
195 lipid-rich conditions when *Mtb* H37Rv reaches stationary phase (Rodriguez, et al. 2014).
196 This important result suggests that exogenous FFA, but not glucose, would be the stimulus
197 responsible for TAG accumulation in *Mtb* and that the physiological mechanisms governing
198 ILI formation in mycobacteria might be well conserved and dependent on the entry into the
199 stationary phase. Importantly, conversion and storage of FFA into TAG appears as a
200 fundamental process, which is conserved from bacteria to human. In particular, it is now
201 well established that lipid droplet storage in eukaryotic cells is a dedicated biological
202 mechanism that prevents lipotoxicity through excessive reactive oxygen species generation
203 during FFA diet (Listenberger, et al. 2003).

204 Alternatively, when mycobacterial species such as *Msmeg* were exposed to a high
205 concentration of glycerol and in absence of FFA as a lipid source, ILI accumulation was
206 observed during the stationary phase and monitored by thin layer chromatography (TLC)
207 and microscopic approaches (Armstrong, et al. 2016, Armstrong, et al. 2018, Garton, et al.
208 2002, Santucci, et al. 2019a). The significant accumulation of ILI led the authors to propose
209 that the FFA incorporated within TAG-forming inclusions was directly derived from *de novo*
210 synthesis. This is of particular interest since it implies that the two distinct experimental
211 designs mentioned above (*i.e.*, excess of exogenous FFA or high glycerol diet) are perfectly
212 complementary highlighting the potential of easily applying these stimuli to modulate and
213 characterize the pathways involved in ILI biosynthesis.

214

215 II) Nitrogen deprivation

216 Limitation of nitrogen has been well documented as another major cause triggering TAG
217 biosynthesis and ILI formation (Alvarez, et al. 2000, Alvarez, et al. 1996, Garton, et al.
218 2002, Santucci, et al. 2019a). First evidences were observed in *Streptomyces* sp. where the
219 authors noticed an increase in the TAG content upon cultivation under nitrogen-deprived
220 conditions (Olukoshi and Packter 1994). This was further confirmed with the *Rhodococcus*
221 *opacus* strain PD630, capable to produce insoluble inclusions when grown in presence of

222 different hydrocarbon substrates under low nitrogen conditions (Alvarez, et al. 1996).
223 Finally, the fact that *Rhodococcus* cells, grown in a medium with a fixed concentration of
224 carbon source, accumulate increasing amounts of TAG in stationary phase and that this
225 process is inversely proportional to the concentration of ammonium available in the broth
226 medium, clearly supports the assertion that ILI formation *in vitro* is directly correlated with
227 ammonium deprivation (Alvarez, et al. 2000).

228 In *Msmeg*, two-dimensional TLC analysis and fluorescence microscopy also demonstrated
229 that TAG accumulation occurred after several days of growth under nitrogen-limiting
230 conditions (Garton, et al. 2002). Moreover, gas chromatography coupled to mass
231 spectrometry (GC-MS) analysis of the fatty acid profiles of TAG component stored following
232 nitrogen starvation, revealed the presence of an increased proportion of already
233 synthesized saturated FFA resulting from *de novo* synthesis (Garton, et al. 2002).

234 Recently, using defined-minimal media, our group confirmed that carbon excess and
235 nitrogen limitation promote *in vitro* TAG accumulation under the form of ILI in both *Msmeg*
236 and *Mycobacterium abscessus* (*Mabs*) (Santucci, et al. 2019a). Based these findings, it was
237 proposed that the stress responses during nitrogen deprivation may be evolutionarily
238 conserved among different mycobacterial species (Santucci, et al. 2019a).

239 In fact, the biological pathways and specific role of putative conserved molecular factors
240 involved in actinobacterial adaptation to nitrogen starvation have started to be investigated
241 over the last decade (Amon, et al. 2008, Davila Costa, et al. 2017, Jessberger, et al. 2013,
242 Williams, et al. 2015). Among them, the *nlpR* gene, which encodes a master regulator of
243 lipogenesis upon nitrogen starvation in *Rhodococcus jostii* RHA1, has been recently
244 identified as a key player in TAG metabolism (Hernandez, et al. 2017). This gene which is
245 conserved in mycobacterial species such as *Msmeg* and *Mtb* (*MSMEG_0432* and *Rv0260c*
246 genes, respectively) has been demonstrated to be crucial in nitrogen assimilation processes
247 (Jenkins, et al. 2013, Williams, et al. 2015). However, its direct implication in TAG
248 biosynthesis/storage remains elusive. To date, only the mycobacterial PrrAB two-
249 component system has been identified as a negative regulator directly linking nitrogen
250 limitation and TAG accumulation in mycobacteria (Maarsingh and Haydel 2018).
251 Interestingly, deletion of *prrAB* gene in *Msmeg* led to a significant overexpression of the
252 genes encoding enzymes from the Kennedy pathway by which mammalian cells synthesize
253 phospholipids and TAG for incorporation into membranes or lipid-derived signalling
254 molecules, thus favouring TAG accumulation and storage (Maarsingh and Haydel 2018)
255 **(Figure 4).**

256 Altogether, these results underscore conserved pathways involved in adaptation and
257 regulation of lipid metabolism during nitrogen starvation in *Actinobacteria*, and this easy-to-
258 use *in vitro* experimental system combined with molecular genetics and biochemical
259 approaches should further contribute to increase our understanding of these biological
260 pathways.

261

262 III) Hypoxia

263 Mycobacterial species require constant levels of oxygen for growth. However, many studies
264 suggested that the tubercle bacilli encounter hypoxic microenvironments in both active
265 disease as well as during LTBI (Via, et al. 2008, Wayne and Sohaskey 2001). To survive
266 under these specific conditions, *Mtb* uses several adaptive pathways relying on the well-
267 known *dormancy survival regulator* (Dos) regulon, which comprises of approximately 50
268 genes and controlled by the DosRST three-component system (Boon and Dick 2002, Park,
269 et al. 2003, Sherman, et al. 2001). During low oxygen tension, several TGS-encoding
270 genes are upregulated by *Mtb*, among which the *tgs1* (i.e., *rv3130c*) gene being part of the
271 Dos regulon is strongly overexpressed (Daniel, et al. 2004). Genetic disruption of *tgs1*
272 drastically reduces TAG accumulation during gradual depletion of oxygen while *trans*-
273 complementation almost fully restored the WT phenotype, suggesting that *tgs1* is a critical
274 factor in TAG synthesis and accumulation in *Mtb* H37Rv (Sirakova, et al. 2006). As a result,
275 hypoxia-induced TAG accumulation has been acknowledged as a relevant *in vitro* model,
276 termed as the “Wayne” hypoxia model, widely used to dissect the molecular mechanisms
277 involved in ILI formation in *Mtb* and also in other species composing the *Mtb* complex
278 (Levillain, et al. 2017, Low, et al. 2009, Low, et al. 2010). Similar experimental stimuli were
279 successfully applied to the vaccine strain *Mycobacterium bovis* BCG (*Mbv* BCG), showing
280 that *Mbv* BCG was capable to accumulate TAG under the form of ILI during hypoxia but not
281 in aerated culture conditions (Low, et al. 2009). By combining the use of fluorescent FFA,
282 confocal microscopy and high-performance liquid chromatography coupled with mass
283 spectrometry, the authors also demonstrated that low oxygen levels promote esterification
284 of exogenous FFA within TAG (Low, et al. 2009). By performing transposon mutagenesis
285 screening on *Mtb* growth under hypoxia, Baek and Sasseti identified 34 genes involved in
286 mycobacterial growth regulation and lipid metabolism during low oxygen tension (Baek, et
287 al. 2011). Among them, *dosR* and *tgs1* mutants were over-represented, confirming their
288 major contribution in the establishment of *Mtb* persitent-like state. Moreover, they clearly

289 demonstrated that growth reduction upon hypoxia was mediated by Tgs1 and TAG
290 formation by down-regulating the tricarboxylic acid cycle (TCA).

291 More recently, transcriptional studies raised new concepts regarding the role of hypoxia in
292 persistent-like state and dormancy establishment. Indeed, RNA-sequencing results
293 suggested that both the nature of the carbon source (*i.e.*, dextrose or FFA) and oxygen
294 depletion are involved in a successful adaptation leading to TAG accumulation inside ILI
295 (Del Portillo, et al. 2018, Rodriguez, et al. 2014). These observations strongly suggest that
296 hypoxia occurring in damaged tissue during infection may be directly linked to FFA uptake
297 and metabolism within specific microenvironments surrounding the bacilli, and that all act
298 together to promote a lipid-rich phenotype.

299

300 IV) NO exposure

301 In addition to oxygen deprivation, large amounts of NO have been shown to inhibit aerobic
302 respiration and induce non-replicating persistent state. Several studies demonstrated that
303 upon NO treatment, genes from the Dos regulon, including *tgs1*, were significantly
304 upregulated in *Mtb* cultures (Ohno, et al. 2003, Voskuil, et al. 2003). This overexpression
305 was not only associated with an important increase in TAG accumulation, but importantly,
306 NO treatment was also responsible for a greater incorporation of radiolabelled acetate and
307 exogenous FFA into TAG, resulting molecules mainly formed by saturated C16:0 to C28:0
308 acyl chains (Daniel, et al. 2004).

309 This NO stress experimental system has been used recently with the vaccine strain *Mbv*
310 BCG to investigate the contribution of the heparin-binding hemagglutinin adhesin (HBHA) in
311 ILI formation (Raze, et al. 2018). Analysis of the lipid content of *Mbv* BCG WT and $\Delta hbhA$
312 strains by fluorescence and electron microscopy, revealed that deletion of *hbhA* impairs ILI
313 formation upon NO stress (Raze, et al. 2018), while re-introduction of *hbhA* in the mutant
314 strain restored ILI accumulation to levels comparable to those found in the parental strain.
315 This simple induction system, which mimics O₂ depletion, confirms that inhibition of aerobic
316 respiration trigger FFA import and esterification onto TAG molecules inside mycobacteria.

317

318 V) Iron starvation and oxidative stress

319 Iron acquisition and storage has also been reported to play an essential role in *Mtb* survival
320 and virulence (Bacon, et al. 2007). Within the host, making iron unavailable for the
321 pathogens through sequestration or deprivation, represents an important defence

322 mechanism. It has been observed that low level of iron *in vivo* works as a stimulus for the
323 expression of virulence genes in numerous microbial pathogens. In addition, several genes
324 involved in lipid biosynthesis and accumulation are overexpressed in *Mtb* under iron
325 starvation (Rodriguez, et al. 2002). In *Mtb* H37Rv, *in vitro* chemostat cultures under iron-
326 poor conditions led to the accumulation of TAG and the production of an unidentified novel
327 wax ester (WE) (Bacon, et al. 2007, Pal, et al. 2019). Iron depletion could also be achieved
328 with deferoxamine mesylate salt, a powerful iron chelator. Using this approach, the authors
329 demonstrated that *Mtb* H37Rv and several clinical strains were able to produce large
330 amount of ILI (Vijay, et al. 2017). Since these specific starvation conditions are also known
331 to induce an important oxidative stress in cells by increasing the production of radical
332 oxygen species, when *Mtb* H37Rv and several clinical isolates were submitted to increasing
333 concentration of H₂O₂, all strains accumulated TAG under the form of ILI. No additional
334 information regarding this *in vitro* experimental design is available regarding NTM.

335

336 **Enzymatic pathways involved in TAG biosynthesis**

337 If multiple environmental conditions are able to promote ILI formation in actinobacteria, they
338 essentially rely on highly conserved pathways and enzymatic actors to synthesize TAG
339 molecules. From a molecular perspective, these enzymatic reactions can be subdivided into
340 three major steps, which are (i) the production and/or importation of fatty acyl-compounds;
341 (ii) the formation of glycerol intermediates and (iii) the sequential esterification of the
342 glycerol moiety with fatty acyl-residues (Alvarez and Steinbüchel 2002) (Figure 4).

343 The initial step consists in generating fatty acid moieties under the form of acyl-CoA
344 molecules which will be subsequently condensed with glycerol-3-phosphate (G3P)
345 substrates. FFA required for TAG biosynthesis can be either synthesized *de novo* through
346 the action of the type I fatty acid synthetase (FAS-I) or directly imported from the
347 environment *via* multiple transporters. Then, the G3P plays a pivotal role in the biosynthesis
348 of glycerol intermediates, which are required for both membrane glycerophospholipid and
349 TAG metabolism. The intrabacterial pool of G3P is generated by the complementary action
350 of the glycerol kinase, which converts free glycerol into G3P and the G3P dehydrogenase
351 that catalyzes the reduction of dihydroxyacetone phosphate into G3P by using the
352 NAD(P)H cofactor as a reductant. The final step is mediated by the enzymes from the
353 Kennedy pathway which condenses FFA and G3P into lysophosphatidic acid (LPA), and
354 subsequently in phosphatidic acid (PA), DAG and TAG respectively. Despite their
355 physiological and clinical relevance, very few information is available regarding these three
356 major pathways in *Mtb*.

357

358 **Free fatty acids uptake and biogenesis**

359 *De novo* synthesis of FFA in mycobacteria is mediated by the multi-enzymatic complex,
360 FAS-I, which uses acetyl-CoA and malonyl-CoA substrates to elongate fatty acids beyond
361 C16 and up to C24-C26 (Bazet Lyonnet, et al. 2017, Gago, et al. 2019). Thus, FAS-I
362 provides essential FFA precursors that will be used to produce mycolic acids, complex
363 polyketides or TAG (Pawelczyk and Kremer 2014). In addition to *de novo* biosynthesis, it is
364 now commonly acknowledged that the tubercle bacilli are able to acquire host-derived fatty
365 acids and cholesterol which are critical carbon sources required for growth, chronic
366 persistence and reactivation processes (Lovewell, et al. 2016). However, how these highly
367 hydrophobic substrates were able to cross the thick and impermeable mycobacterial cell-
368 wall was unclear until recently. Initial studies reported that mammalian transmembrane
369 proteins involved in lipid acquisition also designated fatty acid transport proteins (FATP)

370 were highly conserved and found in a wide panel of organisms, including *Caenorhabditis*
371 *elegans*, *Drosophila melanogaster*, *Saccharomyces cerevisiae* and *Mtb* (Hirsch, et al.
372 1998). Ectopic overexpression of FACL6/Rv1206 in COS cells revealed that this
373 mycobacterial FATP was able to facilitate FFA uptake, suggesting that this molecular actor
374 might play a key role in lipid import (Hirsch, et al. 1998). Another independent study showed
375 that the purified protein displayed acyl-CoA synthetase activity *in vitro* and heterologous
376 expression in *E. coli* promoted fatty acid uptake/utilization (Daniel, et al. 2014). Moreover,
377 genetic disruption of the gene encoding FACL6 in *Mtb*, showed that this protein is required
378 for optimal incorporation of radiolabeled exogenous fatty acids and the production of
379 intracellular TAG during *in vitro* dormancy (Daniel, et al. 2014). However, these findings
380 failed to directly demonstrate that FACL6 acts as fatty acid transmembrane transporter
381 *stricto sensu*.

382 In their seminal work, Pandey and Sasseti clearly demonstrated that *Mtb* imports
383 cholesterol across the cell envelope by using the multi-subunit Mce transporter, Mce4
384 (Pandey and Sasseti 2008). Interestingly, *Mtb* genome contains four unlinked *mce* loci
385 (*mce1-mce4*), which encode numerous proteins of unknown functions, nevertheless, the
386 similarities among the 4 loci indicate that all of them might be transporters required to
387 import hydrophobic molecules (Cole, et al. 1998, Ekiert, et al. 2017, Pandey and Sasseti
388 2008). Recently, Nazarova and colleagues identified Mce1 as *Mtb*'s main machinery
389 involved in fatty acid import *in vitro* and *in cellulo* (Nazarova, et al. 2017). They also showed
390 that LucA/Rv3723, plays a central role in exogenous carbon acquisition by facilitating both
391 fatty acid and cholesterol uptake across the cell envelope by stabilizing protein subunits of
392 the Mce1 and Mce4 transporters, respectively (Nazarova, et al. 2017). As expected,
393 deletion of *lucA* led to important growth defects within mouse and human macrophages,
394 fitness reduction in infected mice and decrease in lung inflammation, highlighting the
395 importance of this molecular determinant in *Mtb* pathogenesis.

396

397 ***Biosynthesis of LPA, PA and DAG precursors***

398 Modulation of the environmental conditions triggers bacterial metabolism reprogramming at
399 transcriptional, translational and post-translational levels. In this context, the synthesis of
400 TAG requires the upregulation of genes encoding key enzymes involved in the production
401 of lipid precursors, such as proteins from the Kennedy pathway (Amara, et al. 2016, Chen,
402 et al. 2014, Juarez, et al. 2017). This pathway is composed of four enzymatic reactions that
403 act sequentially to generate TAG molecules from G3P and FFA substrates. (Figure 4)

404 Firstly, the enzyme glycerol-3-phosphate acyltransferase (GPAT) condenses FFA onto
405 G3P. In bacteria, this reaction is performed by the highly conserved PlsB protein which is
406 an essential enzyme involved in phospholipid biogenesis (Feng and Cronan 2011, Noga, et
407 al. 2020). *Mtb* possesses two *plsB* genes encoding putative GPAT proteins named
408 PlsB1/Rv1551 and PlsB2/Rv2482c respectively (Cole, et al. 1998) and still little is known
409 about the function of these two proteins. However, heterologous expression of
410 *plsB1/Rv1551* in *E. coli*, resulted in higher level of glycerophospholipids and cardiolipin
411 when stimulated with exogenous fatty acids suggesting that Rv1551 is a functional GPAT
412 (Law and Daniel 2017).

413 Secondly, the LPA must be converted into PA by an acylglycerol-3-phosphate
414 acyltransferase (AGPAT). In *Mtb* genome, one gene named *Rv2182c* has been annotated
415 as encoding a putative AGPAT (Cole, et al. 1998). Interestingly, several whole-genome
416 mutagenesis experiments revealed that this gene is essential for *Mtb* growth *in vitro*
417 (DeJesus, et al. 2017, Griffin, et al. 2011, Sasseti, et al. 2003) and bioinformatic analysis
418 showed that it possesses numerous orthologs in a wide range of mycobacterial species
419 emphasizing that such molecular determinant might play an important role in mycobacterial
420 physiology. Alternatively, another putative AGPAT was identified associated to the ILI
421 fraction obtained from *Mbov* BCG ILI upon growth in oxygen-limiting conditions. Indeed, the
422 protein BCG1489c (which shares 100% identity with *Mtb* Rv1428c protein) has been
423 described for containing a PlsC-like domain which might be responsible for AGPAT activity.
424 Deletion of the gene *BCG1489c* resulted in a noticeable decrease in TAG accumulation
425 under hypoxia when analysed by TLC, suggesting that this gene is required for optimal
426 TAG synthesis (Low, et al. 2010).

427 Thirdly, the phosphate group from PA has to be cleaved from the substrate backbone by
428 the action of a phosphatidic acid phosphatase (PAP) to generate DAG. This enzymatic
429 reaction is mainly performed by protein belonging to the PAP2 superfamily. Indeed, two
430 proteins from *Streptomyces coelicolor* named Lpp α (SCO1102) and Lpp β (SCO1753) were
431 identified as PAP enzymes involved in TAG accumulation (Comba, et al. 2013).
432 Surprisingly, bioinformatic analysis revealed that only one of these two proteins is
433 conserved in *Mtb*. The protein Rv0308 which is annotated as a putative conserved integral
434 membrane protein, possesses C-terminus region similar to C-terminus of other integral
435 membrane proteins or phosphatases (Cole, et al. 1998). Therefore, this protein might play
436 an important role in ILI formation and other metabolic processes, however no experimental
437 data are available regarding its physiological function.

439 TAG biosynthesis and ILI formation

440 The final and limiting step governing TAG synthesis is mediated by the key enzymes DGAT
441 also known as TGS. Since the identification of the first DGAT (named AtfA) in *Acinetobacter*
442 *calcoaceticus* ADP1 (Kalscheuer and Steinbuchel 2003), homologs from different
443 microorganisms have been identified in multiple genome databases. However, the
444 homology is mainly restricted to certain groups of bacteria, especially actinomycetes, like
445 *Mycobacterium*, *Rhodococcus* and *Streptomyces*, correlating with previous reports on
446 bacterial TAG and WE accumulation processes (Alvarez and Steinbüchel 2002,
447 Wältermann and Steinbüchel 2005). The laboratory strain *Mtb* H37Rv possesses 15 AtfA
448 homologous proteins (Daniel, et al. 2004, Kalscheuer and Steinbuchel 2003, Sirakova, et
449 al. 2006). *In silico* analysis showed that among these 15 proteins, 11 contain the HHxxxDG
450 active-site motif, required for the acyl-CoA acyltransferase activity involved in TAG
451 synthesis, whereas the 4 remaining have modified active-site motifs without any typical
452 consensus sequence. Comprehensive investigation by heterologous production in *E. coli*
453 and determination of total lysate-associated TGS activity showed that all TGS displayed
454 activity *in vitro*. The authors reported that 4 proteins exhibited higher specific activities,
455 these enzymes were then renamed Tgs1-Tgs4 (Daniel, et al. 2004). In addition to these
456 biochemical studies, genetic disruption coupled phenotypic assays allowed to determine
457 that Tgs1 is the main contributor to TAG synthesis and the most active enzyme in *Mtb* in
458 multiple *in vitro* models (Daniel, et al. 2004, Daniel, et al. 2011, Sirakova, et al. 2006).

459 Similarly, in *Mabs* seven Tgs-encoding genes were identified based on the presence of the
460 HHxxxDG motif, among which Tgs1 was also found to be most active protein (Viljoen, et al.
461 2016). Site directed mutagenesis revealed that His144 and Gln145 are essential for
462 enzymatic activity of Tgs1 in this species. Tgs1 could use a range of acyl-CoAs as fatty acyl
463 donors however it is more active in presence of palmitoyl-CoA (Viljoen, et al. 2016). In an
464 independent study, it was shown the heterologous overproduction of *Mtb* mycolyltransferase
465 Ag85A in *Msmeg* led to altered cell morphology, impaired division and the formation of ILI
466 suggesting a possible role of Ag85A in TAG metabolism and ILI biosynthesis (Elamin, et al.
467 2011).

468 In lipid-poor conditions, these enzymes are mainly localized in the membrane fraction
469 (Elamin, et al. 2011, Hayashi, et al. 2016, Viljoen, et al. 2016) supporting previous studies
470 suggesting that TAG biosynthesis is initiated in the inner leaflet of the cytoplasmic
471 membrane before being released into the bacterial cytosol (Waltermann, et al. 2005).

472 Indeed, lipid inclusions synthesis analysis *in vitro* and in *Rhodococcus opacus* PD630
473 demonstrated that TAG is first stored in the form of small lipid inclusions, which remain
474 associated to the cytoplasmic membrane. Then, these small inclusions conglomerated to
475 newly form pre-lipid inclusions which are then released into the cytoplasm as mature ILI
476 with a large amount of associated proteins (Waltermann, et al. 2005) (Figure 4B)

477

478 ***ILI-associated proteomes, structural proteins and anchoring properties***

479 The first isolation of ILI in Actinobacteria was achieved by phase separation following
480 centrifugation in density gradients (Alvarez, et al. 1996), a simple and efficient protocol
481 which had been previously developed to purify polyester(s) granules from *Pseudomonas*
482 *oleovorans* (Preusting, et al. 1993). After isolation, samples were analysed by
483 polyacrylamide gel electrophoresis, and the presence of numerous ILI-associated proteins
484 was observed suggesting that ILI are not only constituted by lipid material (Alvarez, et al.
485 1996).

486 This experimental approach was subsequently optimized to identify proteins associated to
487 the TAG-containing fractions by LC-MS and bioinformatic analysis (Chen, et al. 2014, Ding,
488 et al. 2012). This led to the identification of 228 and 177 proteins *Rhodococcus jostii* RHA1
489 and *Rhodococcus opacus* PD630 ILI proteomes, respectively. *In silico* analyses revealed
490 that, among many proteins belonged to distinct families involved in various processes,
491 including enzymatic, transport, cell-division, transcription/translation processes and proteins
492 with unknown functions (Chen, et al. 2014, Ding, et al. 2012).

493 With respect mycobacterial, only two independent investigations have been carried out in
494 order to identify possible ILI-associated proteins (Armstrong, et al. 2018, Low, et al. 2010).
495 The original study performed by Low and colleagues identified six novel proteins bound to
496 an ILI-enriched fraction from the vaccine strain *Mbv* BCG cultivated under oxygen limiting
497 conditions (Low, et al. 2010). Among them, the authors found the well-characterised Tgs1
498 (BCG3153c/Rv3130c) and Tgs2 (BCG3794c/Rv3734c) proteins, the heat shock protein
499 hspX (BCG2050c/Rv2031c), a putative acylglycerol-phosphate acyltransferase
500 (BCG1489c/Rv1428c), a putative bifunctional long chain acyl-CoA synthase-lipase
501 (BCG1721/Rv1683) as well as a protein with unknown function (BCG1169c/Rv1109c).
502 Heterologous expression of these genes in yeast showed that the corresponding proteins
503 were indeed targeted to ILI, and overexpression/inactivation of the corresponding genes,

504 followed by TLC analysis, confirmed that five of these genes were required for optimal TAG
505 accumulation during hypoxia-induced persistence (Low, et al. 2010).

506 Lately, a complementary study was performed in the saprophytic species *Msmeg* and the
507 enrichment in ILI-associated proteins was analysed upon growth in glycerol-rich Sauton's
508 medium. In this experimental setting, the authors found more than 400 proteins associated
509 to the purified lipid fraction (Armstrong, et al. 2018).

510 While these results obtained in *Msmeg* were similar to those from *Rhodococcus*, it is still
511 not well understood why there are so many differences regarding protein abundance
512 between these two studies. Multiple factors including the experimental growth conditions,
513 but also species-specific features could be responsible for such striking differences.
514 Unfortunately, the biological reason(s) responsible for these discrepancies remain
515 unknown. Moreover, one obvious limitation in these biological settings is the requirement of
516 bacterial cell-lysis which can lead to massive *trans*-contamination of the lipid fraction with
517 highly hydrophobic or membrane proteins, thus generating a large number of false
518 positives. In that context, the development of next-generation, non-invasive approaches
519 such as proximity labelling proteomics will be of great interest for a spatio-temporal
520 description of the protein composition of ILI in mycobacteria. It is now well acknowledged
521 that ILI are constituted by structural proteins that play a critical role in TAG homeostasis by
522 modulating ILI size, shape but also fusion/fission events. To date, three major proteins have
523 been extensively characterised as key structural factor involved in ILI
524 formation/maintenance in mycobacteria.

525 Initially discovered by performing an elegant genetic screening for TAG deficient mutants,
526 *tadA* was identified as an important factor requested for TAG accumulation in *R. opacus*
527 PD630. This highly conserved actinobacterial gene encodes a protein which contains a C-
528 terminal domain belonging to the heparin-binding hemagglutinin family and has been
529 described for regulating ILI size/shape (Ding, et al. 2012, MacEachran, et al. 2010). Indeed,
530 deletion of this gene, triggered an important reduction of ILI size which can be restored by
531 *trans*-complementation (MacEachran, et al. 2010). Interestingly, complementation with a
532 truncated version devoid of the C-terminal domain was unable to phenocopy the WT strain
533 suggesting a key role of this lysine-rich heparin-binding domain in ILI storage (MacEachran,
534 et al. 2010). Similar results were recently generated with its mycobacterial ortholog, HbhA,
535 highlighting a potential conserved structural function (Raze, et al. 2018).

536 Within eukaryotic cells, major structural proteins involved in LD biosynthesis, maintenance
537 and degradation are perilipins also known as PLIN. This family is constituted of proteins that

538 associate with the surface of LD and regulate numerous metabolic processes, impacting the
539 intracellular LD number, shape and size (Kimmel and Sztalryd 2016). Daniel and
540 colleagues, identified a *Mtb* protein (PPE15) which was overproduced under *in vitro*
541 multiple-stress conditions inducing non-replicating persistence and displaying sequence
542 similarity with the mammalian perilipin-1 protein (PLIN1) (Daniel, et al. 2016). Genetic
543 inactivation and TLC analysis showed that *ppe15/rv1039c* is required for TAG accumulation
544 (Daniel, et al. 2016). In addition, fluorescence microscopy revealed that the *ppe15* mutant
545 failed to form Nile-Red positive granules within the well-established *in vitro* multiple-stress
546 model and *in vitro* human granulomas, thus emphasising a critical role in ILI storage in
547 numerous experimental model (Daniel, et al. 2016).

548 Upon characterisation of the ILI-associated proteome in *Rhodococcus*, Ding et al., identified
549 another molecular actor that was overrepresented at the surface of ILI (Ding, et al. 2012).
550 This protein named PspA is homolog to the phage shock protein A of *E. coli* which is
551 involved the plasma membrane maintenance and homeostasis under stress (Joly, et al.
552 2010). Surprisingly, deletion of *pspA* resulted in the formation of supersized ILI and an
553 opposite phenotype was reported upon inactivation of its mycobacterial ortholog
554 *pspA/MSMEG_2695* in *Msmeg* (Armstrong, et al. 2016, Ding, et al. 2012). Despite these
555 conflicting observations, this clearly demonstrates that PspA is an important protein in ILI
556 homeostasis (Armstrong, et al. 2016, Ding, et al. 2012).

557 These three mycobacterial proteins which exert different effects on ILI number, size and
558 shape, however share some key interesting features regarding their subcellular localisation.
559 PPE15, HbhA and PspA proteins have been described for being either membrane-
560 associated (Kobayashi, et al. 2007), exported (Raze, et al. 2018), or secreted *via*
561 macromolecular machineries (Chen, et al. 2017). Strikingly, these proteins are also located
562 at the ILI surface in *Msmeg* (Armstrong, et al. 2018). Where these proteins are subcellularly
563 produced, how they dynamically alternate between intra- and extra-cellular localisation and
564 what the physiological role(s) of these dual localisations are, remain to be fully addressed.
565 Recently, it has been proposed that a small conserved domain might be responsible for the
566 targeting of these determinants at the surface of ILI (Armstrong, et al. 2018). Indeed, the
567 presence of a specific domain either in N-terminal or C-terminal seems critically required for
568 facilitating ILI localisation. Regarding HbhA, it has been shown that its C-terminal domain,
569 which shares also similarities with the apolipoprotein A1/A4/E protein, was responsible for
570 ILI anchoring and aggregation *in vitro* (Ding, et al. 2012, MacEachran, et al. 2010).

571 Based on *in silico* analysis, it was hypothesized that some conserved domains of the
572 PPE15 protein, which are conserved in multiple PLIN, would potentially be responsible for
573 its interaction with ILI, notably *via* its C-terminal hydrophobic region. However, no
574 experimental validation supporting this issue has been performed yet (Daniel, et al. 2016).
575 More recently, an in-depth characterisation of the PspA binding properties allowed to define
576 a putative conserved biochemical pattern that would facilitate proteins interaction with ILI
577 (Armstrong, et al. 2018). Among the five alpha-helix domains (H1 to H5) of PspA, it was
578 reported that the first helix (H1) was necessary and sufficient for subcellular localization of
579 PspA at the ILI surface. The generation and expression of a recombinant GFP variant fused
580 to one or three N-terminus repeated H1 tag(s) allowed to localise the GFP protein onto ILI
581 (Armstrong, et al. 2018). By combining their proteomic approach, with these observations
582 and bioinformatic analysis, the authors were able to identify and validate that specific
583 amphipathic helices are responsible for binding to the ILI surface inside mycobacteria
584 (Armstrong, et al. 2018). However, to date, there is still no information regarding the
585 spatiotemporal dynamics of this association process at the ILI surface. Such investigation
586 will be of great interest in the coming years to finely decipher how, where and when these
587 proteins interact with ILI and govern their homeostasis.

588

589

590 ***TAG breakdown and pharmacological inhibition of lipolysis***

591 The presence of ILI in mycobacterial cells, and more particularly *Mtb*, has been defined as
592 one of the hallmarks of non-replicating persistent bacilli *in vitro* and *in vivo* (Daniel, et al.
593 2011, Garton, et al. 2002, Garton, et al. 2008). These organelles are considered as one of
594 the main strategies employed by mycobacteria to adapt and survive within drastic
595 environmental conditions by providing a constant and sufficient amount of energy over long
596 period of time.

597 Utilization of the energy stored in TAG requires hydrolysis by hydrolases and lipases to
598 release free fatty acids which in turn are catabolized by β -oxidation (Menendez-Bravo, et al.
599 2017). Depending on their nature and substrate specificity, lipolytic enzymes are commonly
600 divided in four classes such as i) carboxylesterases acting on small and partially water-
601 soluble carboxylester substrates; ii) true lipases hydrolyzing water-insoluble substrates such
602 as MAG, DAG and TAG molecules; iii) phospholipases, acting on phospholipid substrates
603 and iv) cutinase-like proteins consisting of a much more versatile family of enzymes able to
604 degrade a wide range of substrate including carboxylesters, TAG, phospholipids, as well as
605 cutin (Delorme, et al. 2012, Masaki, et al. 2005).

606 In order to constantly provide energy upon long-term persistence or during reactivation,
607 degradation of mycobacterial TAG must be initiated by specific proteins displaying TAG-
608 lipase activity. Pioneer work by Deb *et al.*, reported the presence of the *Mtb* Pro-Glu (PE)
609 protein, encoded by *Rv3097c* and named LipY, which has a C-terminal domain with
610 homology to the hormone-sensitive lipase family and containing the conserved GDSAG
611 motif (Deb, et al. 2006). Biochemical characterization demonstrated that LipY displays TAG
612 hydrolase activity *in vitro* (Deb, et al. 2006). Generation of a *lipY* deficient mutant, showed
613 that TAG utilization upon carbon starvation was significantly decreased, indicating that LipY
614 plays an important role for the hydrolysis of stored TAG. This was further confirmed by
615 heterologous expression in *Msmeg*. However, since this latter species does not encode the
616 ESX-5 secretion system, that allow the secretion of LipY, these results have to be
617 considered with caution (Mishra, et al. 2008, Santucci, et al. 2019b). Interestingly, multiple
618 comparison of full-length LipY with a recombinant variant shortened by its N-terminal PE
619 domain (LipY(Δ PE)), revealed that full-length LipY exhibited reduced TAG-hydrolase
620 activity, suggesting a negative modulation of the activity of LipY by its N-terminal PE
621 domain (Garrett, et al. 2015, Mishra, et al. 2008, Santucci, et al. 2018, Santucci, et al.
622 2019b). Enzymatic characterization of LipY showed that this protein also displays DAG-
623 hydrolase activity, implying that this enzyme may also be involved in another essential step

624 upon TAG breakdown (Santucci, et al. 2019b). In addition to LipY, other *Mtb* enzymes have
625 been reported to display true lipase activity. Among them Rv1984c/Cfp21, which belongs to
626 the cutinase-like family proteins, is able to hydrolyze different substrate including medium-
627 chain carboxylic esters, MAG and TAG (Dedieu, et al. 2013, Schué, et al. 2010).
628 Interestingly, the putative bifunctional long chain acyl-CoA synthase-lipase
629 (BCG1721/Rv1683) has been showed to be involved in TAG degradation (Low, et al. 2010).
630 This enzyme possesses a putative N-terminal lipase and a C-terminal ACSL domain,
631 expressing a TAG-lipase activity when overproduced in *Mbv* BCG or in yeast, and this
632 activity was abolished when S150A a point mutation was introduced in the predicted lipase
633 catalytic site (Low, et al. 2010). A previously uncharacterized membrane-associated protein,
634 annotated as Rv2672/Msh1, was reported to express both lipase and protease activities.
635 This protein, which was mainly conserved among actinomycetes, is required for host-TAG
636 hydrolysis, albeit no investigation regarding intrabacterial lipid consumption was done
637 (Singh, et al. 2017). *Mtb* also encodes one monoacylglycerol lipase named Rv0183 which
638 converts monoacylglycerol into free glycerol and fatty acid, which can be further used as a
639 source of energy (Côtés, et al. 2007). Genetic knock-out of *MSMEG_0220*, the ortholog of
640 *Rv0183* in *Msmeg*, triggers drastic changes in morphology and resulted in important
641 antibiotic susceptibility modifications (Dhouib, et al. 2010) but no information is available
642 regarding ILI metabolism. Altogether, this shows that *Mtb* possesses numerous enzymes
643 required for TAG breakdown and generation of FFA but more investigation is required to
644 comprehensively decipher their respective involvement. Two main experimental strategies
645 have been used *in vitro* to better apprehend the process of lipid consumption in
646 mycobacteria. The first one, is based on a simple series of events and mimics fluctuations
647 from a nutrient-limiting to a nutrient-replete condition. Indeed, once the level of any limiting
648 chemical element, metabolites and/or energetic substrates raises again, bacterial cells
649 initiate a global metabolic reprogramming and rapidly start consuming stored TAG in order to
650 fuel their regrowth. Such an experimental model was used by Low and colleagues to
651 investigate the contribution of ILI hydrolysis during regrowth from hypoxia-induced
652 dormancy (Low, et al. 2009).
653 By monitoring bacterial regrowth, the authors demonstrated that ILI mobilization was
654 required to support *Mbv* BCG regrowth during the transition from hypoxia to normoxia (Low,
655 et al. 2009). Interestingly, Orlistat (Tetrahydrolipstatin; THL), a serine-hydrolase inhibitor
656 known for covalently binding and inhibiting mammalian and bacterial lipolytic enzymes as
657 well as fatty acid synthases, was able to prevent the degradation of TAG and to impair *Mbv*

658 BCG growth resumption (Low, et al. 2009). The same group further employed a THL
659 analogue in an activity-based protein profiling assay to identify the target proteins
660 responsible for TAG hydrolysis upon reactivation of *Mbv* BCG (Ravindran, et al. 2014). This
661 approach unravelled many lipolytic enzymes as potential targets needed for lipid
662 metabolism and re-growth. These include carboxylesterases belonging to the Hormone-
663 Sensitive Lipase Lip-family members (*i.e.*, LipD, LipG, LipH, LipI, LipM, LipN, LipO, LipV,
664 LipW, LipY) and the thioesterase TesA (Deb, et al. 2006, Mishra, et al. 2008, Ravindran, et
665 al. 2014).

666 Nevertheless, it is important to mention that these experiments were performed with the
667 vaccine strain *Mbv* BCG and that the role of TAG hydrolysis during outgrowth following
668 hypoxia is still largely unknown in *Mtb*. Investigating whether such biological process is
669 conserved within both *Mtb* laboratory and clinical strains will be of great interest. It should
670 also be pointed out that such powerful approach, mainly based onto pharmacological
671 inhibition, presents some limitations. The low selectivity of THL and its propensity to block a
672 wide range of mycobacterial enzymes may impact numerous biological processes specially
673 when assessing bacterial growth. In this context, confirmation of the observed phenotypes
674 with a complementary approach such as gene overexpression or inactivation is often
675 required (Low, et al. 2009).

676 The second experimental model mainly relies on carbon starvation, which allows to
677 artificially trigger TAG consumption. This approach has been widely used to investigate the
678 mechanisms and dynamics of ILI hydrolysis by first developing an image-based quantitative
679 method to assess lipolysis and ILI dynamics by time-lapse fluorescence microscopy at the
680 single-bacterial cell level. This specific system combined with a microfluidic disposal
681 allowed to monitor intracellular bacterial lipid levels over time with a high temporal
682 resolution (Dhouib, et al. 2011). In this experimental system, upon carbon deprivation using
683 PBS-induced starvation, *Msmeg* rapidly hydrolyses the stored TAG, which results in a rapid
684 consumption of ILI; and this lipolytic activity was abolished in the presence of THL, as
685 observed by fluorescence microscopy and TLC analysis (Dhouib, et al. 2011). More
686 recently, using an *in vitro* model based on nitrogen starvation followed by carbon
687 deprivation, the relative rate of ILI consumption in *Msmeg* and *Mabs* species was
688 determined (Santucci, et al. 2019a). Moreover, heterologous overexpression of the well-
689 characterized *Mtb* lipase LipY under these conditions led to a significant decrease in TAG
690 content in *Msmeg* (Daleke, et al. 2011, Deb, et al. 2006, Mishra, et al. 2008, Santucci, et al.
691 2019b). Importantly, using a model of infected foamy macrophages (FM), it has been

692 demonstrated that specific lipid deprivation within host-cells triggers rapid LD consumption
693 and subsequently ILI breakdown (Caire-Brandli, et al. 2014, Santucci, et al. 2018). In all
694 cases, addition of the serine-hydrolase inhibitor THL or the oxadiazolone-core compound
695 MmPPOX targeting more specifically *Mtb* lipolytic enzymes belonging to the Lip-family
696 members (Delorme, et al. 2012, Nguyen, et al. 2018, Santucci, et al. 2019b), showed that
697 ILI hydrolysis was dependent on mycobacterial lipolytic enzyme activities (Santucci, et al.
698 2018, Santucci, et al. 2019a). These results support the view that lipolytic enzymes are
699 essential for TAG hydrolysis and can be modulated by pharmacological inhibition (**Figure**
700 **5**). They are also consistent with previous findings reporting the importance of lipolytic
701 enzymes during ILI mobilization, suggesting that these processes are well conserved
702 across fast- and slow-growing mycobacteria (Dhouib, et al. 2011, Low, et al. 2009,
703 Santucci, et al. 2019a).

704 Collectively, the results gained from various experimental systems have led to the common
705 consensus, that mycobacterial species have evolved specific complex biological pathways
706 to detect and protect themselves against a wide range of exogenous stresses, mainly by
707 modulating their metabolic profiles (Kumar, et al. 2011). It is clear that the availability of
708 such *in vitro* experimental models will greatly facilitate our understanding of mycobacterial
709 adaptation, lipid metabolism and pathogenesis in a near future.

710

711 ***TAG-derived FFA and TAG export***

712 Upon ILI degradation, TAG-derived molecules such as DAG, MAG and FFA can be
713 redirected in many biological pathways. To date, it is commonly accepted that FFA are
714 mainly used for β -oxidation, releasing acetyl-CoA and the reduced co-factors NADH and
715 FADH₂ providing energy *via* the TCA cycle and the respiratory chain. However, TAG-
716 derived products may also serve as precursor for membrane phospholipids, mycolic acids
717 or complex lipids such as dimycocerosate esters, thus playing a central role in
718 mycobacterial physiology (Aschauer, et al. 2018, Cabruja, et al. 2017, Lee, et al. 2013,
719 Menendez-Bravo, et al. 2017). Indeed, acyl-CoA molecules react with malonyl-ACP to
720 generate very long chain mero-mycolyl-ACP through the type II fatty acid synthase,
721 ultimately leading to the production of mycolic acids (Cabruja, et al. 2017). FFA degradation
722 also lead to the generation of propionyl-CoA, which can generate methyl-malonyl-CoA
723 through the methyl-malonyl pathway, subsequently utilized to produce methyl-branched

724 lipid for the building blocks of the bacterial cell wall (Lee, et al. 2013, Minnikin, et al. 2002,
725 Russell, et al. 2010).

726 Alternatively, TAG can also be directly exported via the LprG-Rv1410 machinery (Martinot,
727 et al. 2016). If the contribution of such machinery in the context of hypoxia-induced
728 persistence has not been investigated yet, one can speculate that such transport system
729 might be required for optimal regrowth.

730 **Biological systems to study ILI metabolism within host cells**

731 Lipid metabolism is an extremely complex process, particularly during mycobacterial
732 infection which is modulated by numerous factors. Inside granulomas, mycobacteria
733 encounter different extracellular environments and interact with host immune cells. Among
734 the cells, the FM or lipid-loaded macrophages, represent an atypical cell type that has been
735 the subject of intensive research over the last decades (Russell, et al. 2009). Although they
736 might play a critical role in persistence and reactivation of the tubercle bacillus, leading to
737 the spread of the disease, the exact role of these specific cells in mycobacterial
738 pathogenesis remains unclear. Multiple cellular models have been developed to dissect the
739 mechanism by which mycobacteria acquire lipids from the host and use them for
740 synthesizing their own ILI, and to understand how this process influences the outcome of
741 the infection (Barisch and Soldati 2017, Santucci, et al. 2016).

742 Intracellular acquisition and accumulation of lipids from the host was first described in non-
743 immune cells where *Mtb* was able to accumulate ILI and survive in a non-replicating state
744 within adipocytes (Neyrolles, et al. 2006). These results were recently confirmed with
745 *Mycobacterium canettii*, another member of the *Mtb* complex (Bouزيد, et al. 2017).

746 This infection model using adipose cells further allowed to investigate the expression of
747 specific genes required for host-derived lipids consumption and biosynthesis of ILI.
748 Transcriptional studies of *Mtb*-infected adipocytes revealed that the *dosR* gene encoding
749 the master regulator of the dormancy regulon and the *icl* gene encoding the main isocitrate
750 lyase were both highly upregulated (Rastogi, et al. 2016). Moreover, *tgs1* and *tgs2* as well
751 as several genes encoding lipolytic enzymes belonging to the Lip (*lipF*, *lipH*, *lipN*, *lipX* and
752 *lipY*) and cutinase-like (*culp5*, *culp7* and *culp6*) families were also strongly upregulated,
753 thus suggesting an important role of these enzymes in host-derived lipid degradation and
754 accumulation (Rastogi, et al. 2016). In an independent study, transcriptome profiling by
755 RNA-sequencing performed on bacilli from infected adipocytes revealed that genes
756 involved in *de novo* FA synthesis, such as *fas* or *acpA*, were downregulated, whereas those
757 predicted to be involved in TAG biosynthesis were significantly overexpressed. Surprisingly

758 *tgs1* was not listed among them (Nandy, et al. 2018). In addition, no significant differences
759 were observed regarding the expression of lipolytic enzymes at 10 days post-infection,
760 suggesting that temporal changes are an important factor that needs to be considered in
761 this biological system. Importantly, the authors reported the suppression of the transcription
762 factor IdeR, suggesting decreased iron uptake by *Mtb* in the adipocyte model not in
763 preadipocyte infection, in order to prevent oxidative stress (Nandy, et al. 2018). Finally,
764 using an oxidative-sensitive stress on *Mtb* Δ *IdeR* mutant, they showed that incorporation of
765 OA triggers a reduction of the tubercle bacilli cytoplasm and further promote its survival in
766 lipid-rich environment (Nandy, et al. 2018).

767 The first investigations in human immune cells were performed by using an *in vitro* model of
768 mycobacterial granulomas (Peyron, et al. 2008, Puissegur, et al. 2004). In this biological
769 system, peripheral blood mononuclear cells (PBMCs) isolated from the blood of healthy
770 donors were infected with *Mtb* for 3 or 11 days and further processed for conventional
771 electron microscopy (Peyron, et al. 2008). This approach showed how *Mtb* promotes LD
772 formation in *in vitro* human granulomas, but also allowed to describe the fusion events
773 between host-LD and the mycobacterium-containing vacuole. Such observations were also
774 correlated with the presence of ILI, suggesting that ILI formation in *Mtb* might derived from
775 the acquisition of lipids contained within host-LD (Peyron, et al. 2008). Complementary
776 experiments within PBMC-derived macrophages showed that, over time, the bacterial
777 burden within FM was significantly lower in comparison to the one in lipid-poor cells.
778 Transcriptomic analysis revealed that *dosR*, *icl* and *tgs1* genes were massively upregulated
779 during infection of FM, suggesting that foamy PBMCs may provide a niche for *Mtb* long-
780 term persistence in a lipid-rich non-replicating state (Peyron, et al. 2008). Interestingly,
781 these observations were further confirmed in both human monocytic cell line THP-1 and
782 PBMC-derived macrophages exposed to 1% of O₂ (Daniel, et al. 2011). In such a hypoxia-
783 based cellular model, the authors used exogenous isotopically labelled FFA followed by
784 TLC analysis to report that *Mtb* assimilated host-derived TAG as a lipid source which was
785 subsequently used to build up ILI in a *tgs1*-dependent manner (Daniel, et al. 2011).
786 However, one cannot exclude that some of the exogenous lipids were directly transferred to
787 the bacteria and might impact ILI formation in this experimental model.

788 They also demonstrated that upon FM infection, *Mtb* lost acid fastness and became Nile-
789 Red positive, two well-acknowledged features of non-replicating persistent bacilli (Daniel, et
790 al. 2011). This transition from acid fast-positive to acid fast-negative and Nile-red positive
791 has been shown to be *tgs1*-dependent in an *in vitro* model of granuloma. Additionally, such

792 phenotype was associated to an increase tolerance to the front-line drug rifampicin
793 (Kapoor, et al. 2013).

794 To date, this close relationship between loss of acid fastness, low metabolic activity, lipid
795 accumulation and antibiotic susceptibility is still not well understood (Vilcheze and Kremer
796 2017). Although the key players related to acid fast property of mycobacteria remain largely
797 unexplored, the association of mycolic acids and other cell wall-associated (glyco)lipids with
798 acid fast property of *Mtb* was reported, essentially based on genetically defined mutants
799 found to be attenuated in mice. The approach of this study will not only help improving
800 detection of dormant bacilli but also beneficial for future vaccine developments (Vilcheze
801 and Kremer 2017). In addition to Tgs1, the β -ketoacyl-acyl carrier protein synthase KasB,
802 involved in mycolic acid synthesis, could be one of the major actors involved in loss of acid
803 fastness and long-term persistence (Bhatt, et al. 2007, Vilcheze and Kremer 2017,
804 Vilcheze, et al. 2014). Recently, long-term live-cell imaging of *Mtb*-infected human
805 monocytes-derived macrophages allowed to monitor LD content at the single-cell level, and
806 confirmed that *Mtb* replication correlated a decrease in intracellular TAG, suggesting that
807 LD-contained lipids serve as an important carbon source during infection (Greenwood, et al.
808 2019). Unexpectedly, by combining light, electron and ion microscopy imaging, the authors
809 not only demonstrated that the anti-tubercular antibiotic bedaquiline accumulates within
810 host LD, but also that host-lipid consumption is a dynamic process that enhanced the
811 delivery of bedaquiline within *Mtb* (Greenwood, et al. 2019). The cumulative results in
812 human primary cells clearly strengthen the fact that the intricate interplay between
813 mycobacterial and host lipid metabolism plays a crucial role in the mycobacterial lifecycle,
814 antibiotic susceptibility and treatment outcomes (Agarwal, et al. 2020).

815 The use of mouse bone marrow-derived macrophages (BMDM) further emerged as a good
816 alternative to human macrophages by-passing the donor-to-donor variability occurring when
817 working with human blood samples. In addition, BMDM represent a valuable tool to easily
818 investigate/monitor lipid accumulation in cells derived from specific mouse-models with
819 distinct genetic background (Knight, et al. 2018, Podinovskaia, et al. 2013). Thanks to
820 fluorescence microscopy on infected BMDM exposed to OA, *Mtb* was found to promote
821 significantly the retention of the foamy phenotype (Podinovskaia, et al. 2013). Recent
822 results obtained in *Mtb*-infected BMDM suggest that such accumulation of LD would be
823 dependent on the host macrophage activation profile and essentially mediated by the
824 transcription factor hypoxia-inducible factor 1 α (Hif1- α) (Genoula, et al. 2020, Knight, et al.

825 2018). In this biological system, the use of exogenous FA combined with the fluorescent
826 lipid BODIPY-palmitate demonstrated that exogenous lipids can be acquired by the bacteria
827 during macrophage infection (Podinovskaia, et al. 2013). The Mce1/LucA machinery was
828 identified as a key factor in lipid acquisition (Nazarova, et al. 2017). In the presence of the
829 fluorescent lipid BODIPY-palmitate, flow cytometry combined with fluorescence and
830 electron microscopy approaches demonstrated that a *Mtb* Δ lucA::hygR mutant was unable
831 to utilize FFA and cholesterol during BMDM infection, and consequently to accumulate ILI
832 (Nazarova, et al. 2017). The authors further infected BMDM with a mCherry fluorescent
833 transposon mutant library, then pulse-labelled the infected cells with the latter fluorescent
834 substrate and measured bacterial incorporation of BODIPY-palmitate by flow cytometry to
835 identify which alternative *Mtb* genes are involved in FFA uptake and ILI formation
836 (Nazarova, et al. 2019). Intracellular bacteria with BODIPY-low level were isolated and
837 plated on selective agar. Sequencing of the transposon insertion sites confirmed the
838 important role for the Mce1/LucA transporter but also allowed identifying new genes
839 involved in FFA import/metabolism such as *rv0966c*, *rv0200/omamB*, *rv3484/cpsA* or
840 *rv2583c/reIA* (Nazarova, et al. 2019). Such findings clearly support the idea that ILI
841 formation derives from the dynamic acquisition of host-lipids. It is however important to
842 specify that direct acquisition of labelled lipids by *Mtb* cannot be ruled out and might have
843 also occurred in that biological system.

844 Another experimental system using BMDM as model was developed to investigate how
845 mycobacteria acquire lipids from their hosts. Here, infection with pathogenic mycobacteria
846 is first performed allowing active replication of the bacilli inside infected cells, then infected
847 BMDM are further exposed for 24h to TAG-rich very low density lipoprotein (VLDL) as a
848 lipid source (Caire-Brandli, et al. 2014). Such alternative exogenous lipid source was
849 selected since it requires CD36-mediated internalisation and endolysosomal processing
850 before promoting the appearance of LD in the infected cells. This model was developed in
851 order to limit the exposure of intracellular mycobacteria to exogenous FFA which rapidly
852 diffuse across membranes and the endolysosomal network (Caire-Brandli, et al. 2014). By
853 combining this model with quantitative analysis of EM observations, it was shown that LD
854 rapidly fuse with the *Mav*-containing phagosome, which was associated with an increase in
855 ILI levels (Caire-Brandli, et al. 2014). Upon VLDL treatment intracellular mycobacteria
856 displayed a thinned cell wall, became elongated and the quantification of bacterial septum
857 in addition to CFU scoring demonstrated that mycobacterial division was arrested (Caire-
858 Brandli, et al. 2014). Conversely, upon VLDL removal, both host LD and ILI abundance

859 sharply decreased, suggesting an increase in lipolysis that was correlated with a
860 simultaneous resumption of mycobacterial division (Caire-Brandli, et al. 2014). This *in vitro*
861 FM model was subsequently used to investigate how *Mbv* BCG acquires host lipids in the
862 phagosomal lumen (Santucci, et al. 2018). Deletion and overexpression of the *lipY* gene,
863 encoding the well-characterized mycobacterial TAG-lipase, revealed that, while LipY plays
864 an important role in extra-bacterial lipid consumption, this lipase is not essential for ILI
865 formation within FM (Santucci, et al. 2018). In addition to slow- growing mycobacteria, this
866 model has also been used to investigate the intracellular behaviour of the emerging
867 pathogen *Mabs* within FM (Viljoen, et al. 2016). The authors demonstrated that *Mabs* is
868 able to interact with host-LD and synthesize ILI in a Tgs1-dependent manner (Viljoen, et al.
869 2016).

870 Alternatively, the dynamics of host-lipid consumption and accumulation under the form of ILI
871 was studied during the infection of the amoeba *Dictyostelium discoideum* with the fish
872 pathogen *Mycobacterium marinum* (*Mmar*) (Barisch, et al. 2015, Barisch and Soldati 2017).
873 This system, based on the exogenous addition of FFA to promote lipid-rich phenotype and
874 initially used to identify new proteins involved in LD synthesis within the amoeba (Du, et al.
875 2013) allowed to monitor in real-time the interaction of host LD with the mycobacterium-
876 containing vacuole by using fluorescence microscopy techniques (Barisch, et al. 2015).
877 Following this approach, the authors showed that perilipin proteins were able to coat
878 cytosolic bacteria in a RD1-dependent manner regardless of the presence or the absence
879 of exogenous FFA (Barisch, et al. 2015). Similar results were observed with the eukaryotic
880 TAG synthase Dgat2, but not Dgat1 (Barisch and Soldati 2017). Upon FFA treatment, TAG
881 production was totally abolished in a *Dictyostelium* mutant lacking both *dgat1* and *dgat2*,
882 but this loss was accompanied with an significant increase in endoplasmic reticulum (ER)
883 membrane proliferation (Barisch and Soldati 2017). Surprisingly, the authors showed that,
884 under these specific conditions, *Mmar* was still able to synthesize its own ILI by depleting
885 the ER-like structures and using host phospholipids as main substrates (Barisch and Soldati
886 2017). Finally, they demonstrated that *Mmar* remained metabolically active and acid-fast
887 positive in that biological system. This suggests that some mechanisms linking lipid
888 accumulation, cell-wall alterations and persistence might be different among mycobacterial
889 species and require to be further investigated.

890 Altogether, these findings highlight the complexity of mycobacterial lipid metabolism within
891 host cells. Observations from the last two decades have raised numerous questions and
892 emerging concepts regarding the acquisition of host-derived lipids by mycobacteria. Still

893 very little is known about the physiological roles and dynamics of LD in the context of
894 bacterial infection. Indeed, how membrane-bound or cytosolic bacteria interact with LD in
895 order to exploit their content, remains to be further explored. In that context, investigating
896 the potential occurrence and contribution of LD-derived lipids acquisition *in vivo* and further
897 deciphering to which extent this consumption process influence *Mtb* pathogenesis and
898 disease progression is of great interest.

899
900

901 ***Beneficial role of ILI metabolism in the mycobacterial lifecycle?***

902 *1) ILI, carbon source and mycobacterial metabolism*

903 Although LD and ILI have been considered as “just fat” organelles for decades, it is now
904 well acknowledged that the biological function of these complex structures goes beyond
905 that simplistic view (Cabruja, et al. 2017, Deb, et al. 2009, Henne 2019, Martinot, et al.
906 2016). In the context of chronic mycobacterial infection, accumulation of TAG within ILI has
907 been proposed to serve as a major source of carbon and energy in non-replicating bacteria
908 (Daniel, et al. 2011, Garton, et al. 2002, Garton, et al. 2008, Peyron, et al. 2008) Indeed,
909 slow and long-term TAG breakdown in the absence of exogenous FFA or *de novo* synthesis
910 provide an important acetyl-CoA pool *via* β -oxidation, which can be rerouted to other
911 metabolic pathways or to sustain ATP production and plasma membrane and cell wall
912 integrity (Cabruja, et al. 2017, Deb, et al. 2009, Martinot, et al. 2016). However, the use and
913 combination of several experimental models have recently shed new insights into additional
914 roles of these dynamic organelles in bacteria. Among these alternative functions, ILI
915 formation has appeared essential to limit the reductive stress and lipotoxicity generated by
916 excess of endogenous FFA (Rodriguez, et al. 2014). During infection, the biosynthesis of
917 TAG and phthiocerol dimycocerosates have been shown to be essential for limiting
918 metabolic stress (Lee, et al. 2013). Similar results have been found in primary fibroblast
919 cells and yeasts where TAG biosynthesis is essential to prevent lipotoxicity and cell death
920 (Garbarino, et al. 2009, Garbarino and Sturley 2009, Listenberger, et al. 2003, Petschnigg,
921 et al. 2009). This implies that, like the eukaryotic LD, ILI might also act as conserved
922 organelles involved in the storage of toxic fatty acids, which must be sequestered during
923 specific conditions to prevent the irreversible damages for the cell (Wältermann and
924 Steinbüchel 2005). Alternatively, storage of evaporation-resistant lipids has been proposed
925 as a bacterial strategy to overcome water deficiency under dehydration, where oxidation
926 would be one of the main mechanisms to produce water molecules (Alvarez, et al. 2004).

927 Recently, it has been demonstrated that ILI contained within the saprophytic strain
928 *Rhodococcus jostii* RHA1 are able to bind to genomic DNA through the action of one ILI-
929 associated protein (Zhang, et al. 2017). Indeed, the authors showed that the protein
930 RHA1_Ro02105, homolog of the mycobacterial HBHA, known for its role in ILI formation
931 when localized intracellularly (Raze, et al. 2018), was able to bind and stabilize DNA, thus
932 enhancing bacterial survival under genotoxic stresses (Zhang, et al. 2017). Interestingly,
933 interactions of LD with nucleic acid or histone proteins have also been reported in
934 mammalian cells (Layerenza, et al. 2013, Uzbekov and Roingeard 2013). Despite the fact
935 that the biological significance of these interactions remains obscure, one can hypothesize
936 that such processes could be highly conserved and directly involved in DNA maintenance
937 and/or gene expression modulation.

938

939 II) *ILI and disease progression*

940 Another beneficial role of ILI is provided by the observation of lipid-rich bacilli in sputum
941 from TB-positive individuals originated from Gambia and the United-Kingdom, which raised
942 the hypothesis that these structures might play a key role in the transmission of the tubercle
943 bacilli (Garton, et al. 2008). Thus, ILI may favour bacterial survival during the transit from an
944 individual to another and may also help the bacilli to more easily adapt to the environmental
945 pressure encountered in a new host (Garton, et al. 2008). These speculations are also in
946 line with findings regarding the Beijing family of *Mtb* strains (sub-branch of lineage 2 also
947 known as the East Asian lineage), which has been associated with increased epidemic
948 spread and reported to constructively produce high amounts of TAG (Domenech, et al.
949 2017, Reed, et al. 2007, Tong, et al. 2020). To investigate whether ILI accumulation may
950 confer a significant advantage in the establishment and outcomes of infection, zebrafish
951 embryos were infected with lipid-rich and lipid-poor *Mabs* (Santucci, et al. 2019a).
952 Comparison of the bacterial loads, inflammatory response and larval survival indicated that
953 the lipid-rich persistent-like phenotype favoured bacterial replication and significantly
954 increased the number of granulomatous lesions per fish which is in agreement with a
955 previous study obtained with non-replicating *Mtb* in CB6F1 mice (Dietrich, et al. 2015,
956 Dietrich, et al. 2016, Santucci, et al. 2019a). This was also correlated with an earlier larval
957 mortality, suggesting that pre-existing ILI might confer a specific advantage when colonizing
958 a new host. However, more investigations are required to better understand these important
959 physiopathological aspects. Several studies emphasized that both host and bacterial TAG
960 metabolism are a critical factor influencing and determining the outcome of the infection

961 (Garton, et al. 2008, Jaisinghani, et al. 2018, Kim, et al. 2010, Russell, et al. 2009). A
962 concept of bacterial immunostat lipid-regulated that control host immunopathologic
963 response has been recently proposed (Queiroz and Riley 2017), whereby the synthesis of
964 many different acylated forms of lipid, directly linked to TAG metabolism (Lee, et al. 2013,
965 Singh, et al. 2009) represents a specific strategy used by the tubercle bacilli to decrease
966 the host response and further establish a long-term infection (Queiroz and Riley 2017).

967

968 *III) ILI and antibiotic efficacy*

969 The presence of ILI in mycobacteria has been also reported to drastically impact antibiotic
970 susceptibility which is crucial in the context of bacterial infection. Indeed, non-replicating
971 bacteria with reduced metabolic activity are more tolerant to antibiotic treatments (Baek, et
972 al. 2011, Deb, et al. 2009, Hammond, et al. 2015, Kapoor, et al. 2013, Santucci, et al.
973 2019a). By using an *in vitro* multiple-stress dormancy model, Deb and colleagues showed
974 that specific microenvironments drive the appearance of lipid-loaded, rifampicin and
975 isoniazid-tolerant phenotypes (Deb, et al. 2009). Another complementary study
976 demonstrated that rerouting the carbon flux and TAG synthesis influence both growth rate
977 and antibiotic susceptibility *in vitro* and *in vivo* (Baek, et al. 2011). This was further
978 confirmed by Hammond and colleagues who clearly established a link between the
979 intrabacterial lipid content and drug tolerance in species belonging to the *Mtb* complex as
980 well as in NTM (Hammond, et al. 2015). By discriminating old/young and lipid-rich/poor
981 bacteria, this study raised an interesting concept suggesting that the age of the culture or
982 the growth rate are not always linked to increased tolerance (Hammond, et al. 2015).

983

984 **Concluding remarks and perspectives**

985 It is clear that mycobacterial lipid metabolism, particularly ILI formation and breakdown, are
986 key events that are directly linked to survival, persistence, pathogenicity and drug tolerance.
987 Understanding how the bacilli acquire host lipids, how they metabolise them in order to
988 persist and reactivate remain a fascinating challenge. The combination of genetic,
989 biochemical or pharmacological approaches along with the development of easy-to-use *in*
990 *vitro* biological stimuli and new cellular/animal models is crucial to gain further insights into
991 these physiological processes, inspiring new ways for feeding the discovery of new
992 therapeutic strategies against mycobacterial diseases.

993

994 **Acknowledgements**

995 IM postdoctoral fellowship was funded by the foundation IHU Méditerranée Infection and
996 PS PhD fellowship was funded by the Ministère de l'Enseignement Supérieur, de la
997 Recherche et de l'Innovation. This work was supported by the Centre National de la
998 Recherche Scientifique (CNRS), Aix-Marseille Université (AMU), the ANR grants (LipInTB -
999 19-CE44-0011, ILlome - 20-CE44-0019), the Association Grégory Lemarchal and Vaincre
1000 la Mucoviscidose (project n°RF20160501651), the Université de Montpellier (UM) and the
1001 Institut National de la Santé et de la Recherche Médicale (INSERM).

1002

1003 **Authors contribution**

1004 PS and SC proposed and conceptualized this work. IM, PS and SC wrote the draft of the
1005 manuscript. LK and JFC completed and revised the entire manuscript. IP, VP and LK
1006 provided light and electron microscopy micrographs and helped IM and SC in figures
1007 editing. All authors listed have made a substantial, direct and intellectual contribution to the
1008 work which was supervised by SC. All authors approved the manuscript for publication.

1009

1010 **References**

- 1011 Agarwal P, Combes TW, Shojaee-Moradie F *et al.* Foam Cells Control Mycobacterium tuberculosis Infection.
1012 *Front Microbiol* 2020;**11**: 1394.
- 1013 Alvarez HM. Triacylglycerol and wax ester-accumulating machinery in prokaryotes. *Biochimie* 2016;**120**: 28-
1014 39.
- 1015 Alvarez HM, Kalscheuer R, Steinbuchel A. Accumulation and mobilization of storage lipids by *Rhodococcus*
1016 *opacus* PD630 and *Rhodococcus ruber* NCIMB 40126. *Applied microbiology and biotechnology*
1017 2000;**54**: 218-23.
- 1018 Alvarez HM, Mayer F, Fabritius D *et al.* Formation of intracytoplasmic lipid inclusions by *Rhodococcus opacus*
1019 strain PD630. *Arch Microbiol* 1996;**165**: 377-86.
- 1020 Alvarez HM, Silva RA, Cesari AC *et al.* Physiological and morphological responses of the soil bacterium
1021 *Rhodococcus opacus* strain PD630 to water stress. *FEMS Microbiol Ecol* 2004;**50**: 75-86.
- 1022 Alvarez HM, Steinbüchel A. Triacylglycerols in prokaryotic microorganisms. *Appl Microbiol Biotechnol*
1023 2002;**60**: 367-76.
- 1024 Amara S, Seghezzi N, Otani H *et al.* Characterization of key triacylglycerol biosynthesis processes in
1025 rhodococci. *Sci Rep* 2016;**6**: 24985.
- 1026 Amon J, Brau T, Grimrath A *et al.* Nitrogen control in *Mycobacterium smegmatis*: nitrogen-dependent
1027 expression of ammonium transport and assimilation proteins depends on the OmpR-type regulator
1028 GlnR. *J Bacteriol* 2008;**190**: 7108-16.
- 1029 Armstrong RM, Adams KL, Zilisch JE *et al.* Rv2744c Is a PspA Ortholog That Regulates Lipid Droplet
1030 Homeostasis and Nonreplicating Persistence in *Mycobacterium tuberculosis*. *J Bacteriol* 2016;**198**:
1031 1645-61.
- 1032 Armstrong RM, Carter DC, Atkinson SN *et al.* Association of *Mycobacterium* Proteins with Lipid Droplets.
1033 *Journal of bacteriology* 2018;**200**.
- 1034 Aschauer P, Zimmermann R, Breinbauer R *et al.* The crystal structure of monoacylglycerol lipase from *M.*
1035 *tuberculosis* reveals the basis for specific inhibition. *Sci Rep* 2018;**8**: 8948.

1036 Bacon J, Dover LG, Hatch KA *et al.* Lipid composition and transcriptional response of *Mycobacterium*
1037 tuberculosis grown under iron-limitation in continuous culture: identification of a novel wax ester.
1038 *Microbiology* 2007;**153**: 1435-44.

1039 Baek SH, Li AH, Sassetti CM. Metabolic regulation of mycobacterial growth and antibiotic sensitivity. *PLoS*
1040 *Biol* 2011;**9**: e1001065.

1041 Barisch C, Paschke P, Hagedorn M *et al.* Lipid droplet dynamics at early stages of *Mycobacterium marinum*
1042 infection in *Dictyostelium*. *Cellular microbiology* 2015, DOI 10.1111/cmi.12437.

1043 Barisch C, Soldati T. *Mycobacterium marinum* Degrades Both Triacylglycerols and Phospholipids from Its
1044 *Dictyostelium* Host to Synthesise Its Own Triacylglycerols and Generate Lipid Inclusions. *PLoS*
1045 *pathogens* 2017;**13**: e1006095.

1046 Barksdale L, Kim KS. *Mycobacterium*. *Bacteriol Rev* 1977;**41**: 217-372.

1047 Barry CE, 3rd, Boshoff HI, Dartois V *et al.* The spectrum of latent tuberculosis: rethinking the biology and
1048 intervention strategies. *Nature reviews Microbiology* 2009;**7**: 845-55.

1049 Bazet Lyonnet B, Diacovich L, Gago G *et al.* Functional reconstitution of the *Mycobacterium tuberculosis*
1050 long-chain acyl-CoA carboxylase from multiple acyl-CoA subunits. *FEBS J* 2017;**284**: 1110-25.

1051 Behr MA, Edelstein PH, Ramakrishnan L. Is *Mycobacterium tuberculosis* infection life long? *BMJ* 2019;**367**:
1052 i5770.

1053 Bhatt A, Fujiwara N, Bhatt K *et al.* Deletion of *kasB* in *Mycobacterium tuberculosis* causes loss of acid-
1054 fastness and subclinical latent tuberculosis in immunocompetent mice. *Proc Natl Acad Sci U S A*
1055 2007;**104**: 5157-62.

1056 Bloch H, Segal W. Biochemical differentiation of *Mycobacterium tuberculosis* grown in vivo and in vitro. *J*
1057 *Bacteriol* 1956;**72**: 132-41.

1058 Boon C, Dick T. *Mycobacterium bovis* BCG response regulator essential for hypoxic dormancy. *J Bacteriol*
1059 2002;**184**: 6760-7.

1060 Bouzid F, Bregeon F, Poncin I *et al.* *Mycobacterium canettii* Infection of Adipose Tissues. *Front Cell Infect*
1061 *Microbiol* 2017;**7**: 189.

1062 Brieger EM, Glauert AM. Electron microscopy of the leprosy bacillus: a study of submicroscopical structure.
1063 *Tubercle* 1956a;**37**: 195-206.

1064 Brieger EM, Glauert AM. Sporelike structures in the tubercle bacillus. *Nature* 1956b;**178**: 544.

1065 Burdon KL. Disparity in appearance of true Hansen's bacilli and cultured leprosy bacilli when stained for fat. *J*
1066 *Bacteriol* 1946;**57**: 679-80.

1067 Cabruja M, Mondino S, Tsai YT *et al.* A conditional mutant of the fatty acid synthase unveils unexpected cross
1068 talks in mycobacterial lipid metabolism. *Open Biol* 2017;**7**.

1069 Caire-Brandli I, Papadopoulos A, Malaga W *et al.* Reversible Lipid Accumulation and Associated Division
1070 Arrest of *Mycobacterium avium* in Lipoprotein-Induced Foamy Macrophages May Resemble Key
1071 Events during Latency and Reactivation of Tuberculosis. *Infection and immunity* 2014;**82**: 476-90.

1072 Chen X, Cheng HF, Zhou J *et al.* Structural basis of the PE-PPE protein interaction in *Mycobacterium*
1073 tuberculosis. *J Biol Chem* 2017;**292**: 16880-90.

1074 Chen Y, Ding Y, Yang L *et al.* Integrated omics study delineates the dynamics of lipid droplets in *Rhodococcus*
1075 *opacus* PD630. *Nucleic Acids Res* 2014;**42**: 1052-64.

1076 Cole ST, Brosch R, Parkhill J *et al.* Deciphering the biology of *Mycobacterium tuberculosis* from the complete
1077 genome sequence. *Nature* 1998;**393**: 537-44.

1078 Comba S, Menendez-Bravo S, Arabolaza A *et al.* Identification and physiological characterization of
1079 phosphatidic acid phosphatase enzymes involved in triacylglycerol biosynthesis in *Streptomyces*
1080 *coelicolor*. *Microb Cell Fact* 2013;**12**: 9.

1081 Côtes K, Dhoub R, Douchet I *et al.* Characterization of an exported monoglyceride lipase from
1082 *Mycobacterium tuberculosis* possibly involved in the metabolism of host cell membrane lipids.
1083 *Biochem J* 2007;**408**: 417-27.

1084 Daleke MH, Cascioferro A, de Punder K *et al.* Conserved Pro-Glu (PE) and Pro-Pro-Glu (PPE) protein domains
1085 target LipY lipases of pathogenic mycobacteria to the cell surface via the ESX-5 pathway. *J Biol Chem*
1086 2011;**286**: 19024-34.

1087 Daniel J, Deb C, Dubey VS *et al.* Induction of a novel class of diacylglycerol acyltransferases and triacylglycerol
1088 accumulation in *Mycobacterium tuberculosis* as it goes into a dormancy-like state in culture. *J*
1089 *Bacteriol* 2004;**186**: 5017-30.

1090 Daniel J, Kapoor N, Sirakova T *et al.* The perilipin-like PPE15 protein in *Mycobacterium tuberculosis* is
1091 required for triacylglycerol accumulation under dormancy-inducing conditions. *Molecular*
1092 *microbiology* 2016, DOI 10.1111/mmi.13422.

1093 Daniel J, Maamar H, Deb C *et al.* *Mycobacterium tuberculosis* uses host triacylglycerol to accumulate lipid
1094 droplets and acquires a dormancy-like phenotype in lipid-loaded macrophages. *PLoS Pathog* 2011;**7**:
1095 e1002093.

1096 Daniel J, Sirakova T, Kolattukudy P. An acyl-CoA synthetase in *Mycobacterium tuberculosis* involved in
1097 triacylglycerol accumulation during dormancy. *PLoS ONE* 2014;**9**: e114877.

1098 Davila Costa JS, Silva RA, Leichert L *et al.* Proteome analysis reveals differential expression of proteins
1099 involved in triacylglycerol accumulation by *Rhodococcus jostii* RHA1 after addition of methyl
1100 viologen. *Microbiology* 2017;**163**: 343-54.

1101 Deb C, Daniel J, Sirakova TD *et al.* A novel lipase belonging to the hormone-sensitive lipase family induced
1102 under starvation to utilize stored triacylglycerol in *Mycobacterium tuberculosis*. *J Biol Chem*
1103 2006;**281**: 3866-75.

1104 Deb C, Lee CM, Dubey VS *et al.* A novel in vitro multiple-stress dormancy model for *Mycobacterium*
1105 *tuberculosis* generates a lipid-loaded, drug-tolerant, dormant pathogen. *PLoS One* 2009;**4**: e6077.

1106 Dedieu L, Serveau-Avesque C, Canaan S. Identification of residues involved in substrate specificity and
1107 cytotoxicity of two closely related cutinases from *Mycobacterium tuberculosis*. *PLoS ONE* 2013;**8**:
1108 e66913.

1109 DeJesus MA, Gerrick ER, Xu W *et al.* Comprehensive Essentiality Analysis of the *Mycobacterium tuberculosis*
1110 Genome via Saturating Transposon Mutagenesis. *MBio* 2017;**8**.

1111 Del Portillo P, Garcia-Morales L, Menendez MC *et al.* Hypoxia Is Not a Main Stress When *Mycobacterium*
1112 *tuberculosis* Is in a Dormancy-Like Long-Chain Fatty Acid Environment. *Front Cell Infect Microbiol*
1113 2018;**8**: 449.

1114 Delorme V, Diomande SV, Dedieu L *et al.* MmPPOX Inhibits *Mycobacterium tuberculosis* Lipolytic Enzymes
1115 Belonging to the Hormone-Sensitive Lipase Family and Alters Mycobacterial Growth. *PLoS ONE*
1116 2012;**7**: e46493.

1117 Dhouib R, Ducret A, Hubert P *et al.* Watching intracellular lipolysis in mycobacteria using time lapse
1118 fluorescence microscopy. *Biochim Biophys Acta* 2011;**1811**: 234-41.

1119 Dhouib R, Laval F, Carriere F *et al.* A monoacylglycerol lipase from *Mycobacterium smegmatis* Involved in
1120 bacterial cell interaction. *J Bacteriol* 2010;**192**: 4776-85.

1121 Dietrich J, Roy S, Rosenkrands I *et al.* Differential influence of nutrient-starved *Mycobacterium tuberculosis*
1122 on adaptive immunity results in progressive tuberculosis disease and pathology. *Infect Immun*
1123 2015;**83**: 4731-9.

1124 Dietrich J, Roy S, Rosenkrands I *et al.* Correction for Dietrich et al., Differential Influence of Nutrient-Starved
1125 *Mycobacterium tuberculosis* on Adaptive Immunity Results in Progressive Tuberculosis Disease and
1126 Pathology. *Infect Immun* 2016;**84**: 608.

1127 Ding Y, Yang L, Zhang S *et al.* Identification of the major functional proteins of prokaryotic lipid droplets. *J*
1128 *Lipid Res* 2012;**53**: 399-411.

1129 Domenech P, Zou J, Averback A *et al.* Unique Regulation of the DosR Regulon in the Beijing Lineage of
1130 *Mycobacterium tuberculosis*. *J Bacteriol* 2017;**199**.

1131 Du X, Barisch C, Paschke P *et al.* Dictyostelium lipid droplets host novel proteins. *Eukaryot Cell* 2013;**12**:
1132 1517-29.

1133 Ekiert DC, Bhabha G, Isom GL *et al.* Architectures of Lipid Transport Systems for the Bacterial Outer
1134 Membrane. *Cell* 2017;**169**: 273-85 e17.

1135 Elamin AA, Stehr M, Spallek R *et al.* The *Mycobacterium tuberculosis* Ag85A is a novel diacylglycerol
1136 acyltransferase involved in lipid body formation. *Mol Microbiol* 2011;**81**: 1577-92.

1137 Feng Y, Cronan JE. The *Vibrio cholerae* fatty acid regulatory protein, FadR, represses transcription of *plsB*, the
1138 gene encoding the first enzyme of membrane phospholipid biosynthesis. *Mol Microbiol* 2011;**81**:
1139 1020-33.

1140 Gago G, Arabolaza A, Diacovich L *et al.* Components and Key Regulatory Steps of Lipid Biosynthesis in
1141 Actinomycetes. In: Geiger O (ed.) *Biogenesis of Fatty Acids, Lipids and Membranes*, DOI 10.1007/978-
1142 3-319-50430-8_65. Cham: Springer International Publishing, 2019, 409-33.

1143 Garbarino J, Padamsee M, Wilcox L *et al.* Sterol and diacylglycerol acyltransferase deficiency triggers fatty
1144 acid-mediated cell death. *J Biol Chem* 2009;**284**: 30994-1005.

1145 Garbarino J, Sturley SL. Saturated with fat: new perspectives on lipotoxicity. *Curr Opin Clin Nutr Metab Care*
1146 2009;**12**: 110-6.

1147 Garrett CK, Broadwell LJ, Hayne CK *et al.* Modulation of the Activity of Mycobacterium tuberculosis LipY by
1148 Its PE Domain. *PLoS ONE* 2015;**10**: e0135447.

1149 Garton N, Christensen H, Minnikin D *et al.* Intracellular lipophilic inclusions of mycobacteria in vitro and in
1150 sputum. *Microbiology* 2002;**148**: 2951-8.

1151 Garton NJ, Waddell SJ, Sherratt AL *et al.* Cytological and transcript analyses reveal fat and lazy persister-like
1152 bacilli in tuberculous sputum. *PLoS Med* 2008;**5**: e75.

1153 Genoula M, Marin Franco JL, Maio M *et al.* Fatty acid oxidation of alternatively activated macrophages
1154 prevents foam cell formation, but Mycobacterium tuberculosis counteracts this process via HIF-
1155 1-alpha activation. *PLoS Pathog* 2020;**16**: e1008929.

1156 Greenwood DJ, Dos Santos MS, Huang S *et al.* Subcellular antibiotic visualization reveals a dynamic drug
1157 reservoir in infected macrophages. *Science* 2019;**364**: 1279-82.

1158 Griffin JE, Gawronski JD, Dejesus MA *et al.* High-resolution phenotypic profiling defines genes essential for
1159 mycobacterial growth and cholesterol catabolism. *PLoS pathogens* 2011;**7**: e1002251.

1160 Hammond RJ, Baron VO, Oravcova K *et al.* Phenotypic resistance in mycobacteria: is it because I am old or fat
1161 that I resist you? *J Antimicrob Chemother* 2015;**70**: 2823-7.

1162 Hartman TL. The Use of Sudan Black B as a Bacterial Fat Stain. *Stain Technology* 1940;**15**: 23-8.

1163 Hayashi JM, Luo CY, Mayfield JA *et al.* Spatially distinct and metabolically active membrane domain in
1164 mycobacteria. *Proc Natl Acad Sci U S A* 2016;**113**: 5400-5.

1165 Henne M. And three's a party: lysosomes, lipid droplets, and the ER in lipid trafficking and cell homeostasis.
1166 *Curr Opin Cell Biol* 2019;**59**: 40-9.

1167 Hernandez MA, Lara J, Gago G *et al.* The pleiotropic transcriptional regulator NlpR contributes to the
1168 modulation of nitrogen metabolism, lipogenesis and triacylglycerol accumulation in oleaginous
1169 rhodococci. *Mol Microbiol* 2017;**103**: 366-85.

1170 Hirsch D, Stahl A, Lodish HF. A family of fatty acid transporters conserved from mycobacterium to man. *Proc*
1171 *Natl Acad Sci* 1998;**95**: 8625-9.

1172 Honer zu Bentrup K, Russell DG. Mycobacterial persistence: adaptation to a changing environment. *Trends*
1173 *Microbiol* 2001;**9**: 597-605.

1174 Jaisinghani N, Dawa S, Singh K *et al.* Necrosis Driven Triglyceride Synthesis Primes Macrophages for
1175 Inflammation During Mycobacterium tuberculosis Infection. *Front Immunol* 2018;**9**: 1490.

1176 Jenkins VA, Barton GR, Robertson BD *et al.* Genome wide analysis of the complete GlnR nitrogen-response
1177 regulon in Mycobacterium smegmatis. *BMC Genomics* 2013;**14**: 301.

1178 Jessberger N, Lu Y, Amon J *et al.* Nitrogen starvation-induced transcriptome alterations and influence of
1179 transcription regulator mutants in Mycobacterium smegmatis. *BMC Res Notes* 2013;**6**: 482.

1180 Joly N, Engl C, Jovanovic G *et al.* Managing membrane stress: the phage shock protein (Psp) response, from
1181 molecular mechanisms to physiology. *FEMS Microbiol Rev* 2010;**34**: 797-827.

1182 Juarez A, Villa JA, Lanza VF *et al.* Nutrient starvation leading to triglyceride accumulation activates the Entner
1183 Doudoroff pathway in Rhodococcus jostii RHA1. *Microb Cell Fact* 2017;**16**: 35.

1184 Kalscheuer R, Steinbuchel A. A novel bifunctional wax ester synthase/acyl-CoA:diacylglycerol acyltransferase
1185 mediates wax ester and triacylglycerol biosynthesis in Acinetobacter calcoaceticus ADP1. *J Biol Chem*
1186 2003;**278**: 8075-82.

1187 Kapoor N, Pawar S, Sirakova TD *et al.* Human granuloma in vitro model, for TB dormancy and resuscitation.
1188 *PLoS ONE* 2013;**8**: e53657.

1189 Kim MJ, Wainwright HC, Locketz M *et al.* Caseation of human tuberculosis granulomas correlates with
1190 elevated host lipid metabolism. *EMBO Mol Med* 2010;**2**: 258-74.

1191 Kimmel AR, Sztalryd C. The Perilipins: Major Cytosolic Lipid Droplet-Associated Proteins and Their Roles in
1192 Cellular Lipid Storage, Mobilization, and Systemic Homeostasis. *Annu Rev Nutr* 2016;**36**: 471-509.

1193 Knaysi G, Hillier J, Fabricant C. The cytology of an avian strain of Mycobacterium tuberculosis studied with
1194 the electron and light microscopes. *J Bacteriol* 1950;**60**: 423-47.

1195 Knight M, Braverman J, Asfaha K *et al.* Lipid droplet formation in Mycobacterium tuberculosis infected
1196 macrophages requires IFN-gamma/HIF-1alpha signaling and supports host defense. *PLoS Pathog*
1197 2018;**14**: e1006874.

1198 Kobayashi R, Suzuki T, Yoshida M. Escherichia coli phage-shock protein A (PspA) binds to membrane
1199 phospholipids and repairs proton leakage of the damaged membranes. *Mol Microbiol* 2007;**66**: 100-
1200 9.

1201 Kumar A, Farhana A, Guidry L *et al.* Redox homeostasis in mycobacteria: the key to tuberculosis control?
1202 *Expert Rev Mol Med* 2011;**13**: e39.

1203 Larrouy-Maumus G, Biswas T, Hunt DM *et al.* Discovery of a glycerol 3-phosphate phosphatase reveals
1204 glycerophospholipid polar head recycling in Mycobacterium tuberculosis. *Proc Natl Acad Sci U S A*
1205 2013;**110**: 11320-5.

1206 Law JD, Daniel J. The mycobacterial Rv1551 glycerol-3-phosphate acyltransferase enhances phospholipid
1207 biosynthesis in cell lysates of Escherichia coli. *Microb Pathog* 2017;**113**: 269-75.

1208 Layerenza JP, Gonzalez P, Garcia de Bravo MM *et al.* Nuclear lipid droplets: a novel nuclear domain. *Biochim*
1209 *Biophys Acta* 2013;**1831**: 327-40.

1210 Lee W, VanderVen BC, Fahey RJ *et al.* Intracellular Mycobacterium tuberculosis exploits host-derived fatty
1211 acids to limit metabolic stress. *J Biol Chem* 2013;**288**: 6788-800.

1212 Levillain F, Poquet Y, Mallet L *et al.* Horizontal acquisition of a hypoxia-responsive molybdenum cofactor
1213 biosynthesis pathway contributed to Mycobacterium tuberculosis pathoadaptation. *PLoS Pathog*
1214 2017;**13**: e1006752.

1215 Listenberger LL, Han X, Lewis SE *et al.* Triglyceride accumulation protects against fatty acid-induced
1216 lipotoxicity. *Proc Natl Acad Sci U S A* 2003;**100**: 3077-82.

1217 Lovewell RR, Sasseti CM, VanderVen BC. Chewing the fat: lipid metabolism and homeostasis during M.
1218 tuberculosis infection. *Curr Opin Microbiol* 2016;**29**: 30-6.

1219 Low KL, Rao PS, Shui G *et al.* Triacylglycerol utilization is required for regrowth of in vitro hypoxic
1220 nonreplicating *Mycobacterium bovis* bacillus Calmette-Guerin. *J Bacteriol* 2009;**191**: 5037-43.

1221 Low KL, Shui G, Natter K *et al.* Lipid droplet-associated proteins are involved in the biosynthesis and
1222 hydrolysis of triacylglycerol in *Mycobacterium bovis* bacillus Calmette-Guerin. *J Biol Chem* 2010;**285**:
1223 21662-70.

1224 Maarsingh JD, Haydel SE. Mycobacterium smegmatis PrrAB two-component system influences triacylglycerol
1225 accumulation during ammonium stress. *Microbiology* 2018;**164**: 1276-88.

1226 MacEachran DP, Prophete ME, Sinskey AJ. The Rhodococcus opacus PD630 heparin-binding hemagglutinin
1227 homolog TadA mediates lipid body formation. *Appl Environ Microbiol* 2010;**76**: 7217-25.

1228 Martinot AJ, Farrow M, Bai L *et al.* Mycobacterial Metabolic Syndrome: LprG and Rv1410 Regulate
1229 Triacylglyceride Levels, Growth Rate and Virulence in Mycobacterium tuberculosis. *PLoS Pathog*
1230 2016;**12**: e1005351.

1231 Masaki K, Kamini NR, Ikeda H *et al.* Cutinase-like enzyme from the yeast Cryptococcus sp. strain S-2
1232 hydrolyzes polylactic acid and other biodegradable plastics. *Appl Environ Microbiol* 2005;**71**: 7548-
1233 50.

1234 McCarthy C. Utilization of palmitic acid by Mycobacterium avium. *Infect Immun* 1971;**4**: 199-204.

1235 McKinney JD, Honer zu Bentrup K, Munoz-Elias EJ *et al.* Persistence of *Mycobacterium tuberculosis* in
1236 macrophages and mice requires the glyoxylate shunt enzyme isocitrate lyase. *Nature* 2000;**406**: 735-
1237 8.

1238 Menendez-Bravo S, Paganini J, Avignone-Rossa C *et al.* Identification of FadAB Complexes Involved in Fatty
1239 Acid beta-Oxidation in *Streptomyces coelicolor* and Construction of a Triacylglycerol Overproducing
1240 strain. *Front Microbiol* 2017;**8**: 1428.

1241 Minnikin DE, Kremer L, Dover LG *et al.* The methyl-branched fortifications of *Mycobacterium tuberculosis*.
1242 *Chem Biol* 2002;**9**: 545-53.

1243 Mishra KC, de Chastellier C, Narayana Y *et al.* Functional role of the PE domain and immunogenicity of the
1244 *Mycobacterium tuberculosis* triacylglycerol hydrolase LipY. *Infect Immun* 2008;**76**: 127-40.

1245 Monson EA, Trenerry AM, Laws JL *et al.* Lipid droplets and lipid mediators in viral infection and immunity.
1246 *FEMS Microbiol Rev* 2021, DOI 10.1093/femsre/fuaa066.

1247 Murphy DJ. The biogenesis and functions of lipid bodies in animals, plants and microorganisms. *Prog Lipid*
1248 *Res* 2001;**40**: 325-438.

1249 Murphy DJ. The dynamic roles of intracellular lipid droplets: from archaea to mammals. *Protoplasma*
1250 2012;**249**: 541-85.

1251 Nakagawa H, Kashiwabara Y, Matsuki G. Metabolism of triacylglycerol in *Mycobacterium smegmatis*. *J*
1252 *Biochem* 1976;**80**: 923-8.

1253 Nandy A, Mondal AK, Pandey R *et al.* Adipocyte Model of *Mycobacterium tuberculosis* Infection Reveals
1254 Differential Availability of Iron to Bacilli in the Lipid-Rich Caseous Environment. *Infect Immun*
1255 2018;**86**.

1256 Nazarova EV, Montague CR, Huang L *et al.* The genetic requirements of fatty acid import by *Mycobacterium*
1257 *tuberculosis* within macrophages. *Elife* 2019;**8**.

1258 Nazarova EV, Montague CR, La T *et al.* Rv3723/LucA coordinates fatty acid and cholesterol uptake in
1259 *Mycobacterium tuberculosis*. *Elife* 2017;**6**.

1260 Neyrolles O, Hernandez-Pando R, Pietri-Rouxel F *et al.* Is Adipose Tissue a Place for *Mycobacterium*
1261 *tuberculosis* Persistence? *PLoS ONE* 2006;**1**: e43.

1262 Nguyen PC, Delorme V, Benarouche A *et al.* Oxadiazolone derivatives, new promising multi-target inhibitors
1263 against *M. tuberculosis*. *Bioorg Chem* 2018;**81**: 414-24.

1264 Noga MJ, Buke F, van den Broek NJF *et al.* Posttranslational Control of PlsB Is Sufficient To Coordinate
1265 Membrane Synthesis with Growth in *Escherichia coli*. *MBio* 2020;**11**.

1266 Ohno H, Zhu G, Mohan VP *et al.* The effects of reactive nitrogen intermediates on gene expression in
1267 *Mycobacterium tuberculosis*. *Cell Microbiol* 2003;**5**: 637-48.

1268 Olukoshi ER, Packter NM. Importance of stored triacylglycerols in *Streptomyces*: possible carbon source for
1269 antibiotics. *Microbiology* 1994;**140 (Pt 4)**: 931-43.

1270 Pal R, Hameed S, Kumar P *et al.* Understanding lipidomic basis of iron limitation induced chemosensitization
1271 of drug-resistant *Mycobacterium tuberculosis*. *3 Biotech* 2019;**9**: 122.

1272 Pandey AK, Sassetti CM. Mycobacterial persistence requires the utilization of host cholesterol. *Proc Natl*
1273 *Acad Sci U S A* 2008;**105**: 4376-80.

1274 Park HD, Guinn KM, Harrell MI *et al.* Rv3133c/dosR is a transcription factor that mediates the hypoxic
1275 response of *Mycobacterium tuberculosis*. *Mol Microbiol* 2003;**48**: 833-43.

1276 Pawelczyk J, Kremer L. The Molecular Genetics of Mycolic Acid Biosynthesis. *Microbiol Spectr* 2014;**2**:
1277 MGM2-0003-2013.

1278 Petschnigg J, Wolinski H, Kolb D *et al.* Good fat, essential cellular requirements for triacylglycerol synthesis to
1279 maintain membrane homeostasis in yeast. *J Biol Chem* 2009;**284**: 30981-93.

1280 Peyron P, Vaubourgeix J, Poquet Y *et al.* Foamy macrophages from tuberculous patients' granulomas
1281 constitute a nutrient-rich reservoir for *M. tuberculosis* persistence. *PLoS Pathog* 2008;**4**: e1000204.

1282 Podinovskaia M, Lee W, Caldwell S *et al.* Infection of macrophages with *Mycobacterium tuberculosis* induces
1283 global modifications to phagosomal function. *Cell Microbiol* 2013;**15**: 843-59.

1284 Preusting H, Kingma J, Huisman G *et al.* Formation of polyester blends by a recombinant strain of
1285 *Pseudomonas oleovorans*: Different poly(3-hydroxyalkanoates) are stored in separate granules.
1286 *Journal of environmental polymer degradation* 1993;**1**: 11-21.

1287 Puissegur MP, Botanch C, Duteyrat JL *et al.* An in vitro dual model of mycobacterial granulomas to
1288 investigate the molecular interactions between mycobacteria and human host cells. *Cell Microbiol*
1289 2004;**6**: 423-33.

1290 Queiroz A, Riley LW. Bacterial immunostat: Mycobacterium tuberculosis lipids and their role in the host
1291 immune response. *Rev Soc Bras Med Trop* 2017;**50**: 9-18.

1292 Ramakrishnan L. Revisiting the role of the granuloma in tuberculosis. *Nature reviews Immunology* 2012;**12**:
1293 352-66.

1294 Rastogi S, Agarwal P, Krishnan MY. Use of an adipocyte model to study the transcriptional adaptation of
1295 Mycobacterium tuberculosis to store and degrade host fat. *Int J Mycobacteriol* 2016;**5**: 92-8.

1296 Ravindran MS, Rao SP, Cheng X *et al.* Targeting Lipid Esterases in Mycobacteria Grown Under Different
1297 Physiological Conditions Using Activity-based Profiling with Tetrahydrolipstatin (THL). *Mol Cell*
1298 *Proteomics* 2014;**13**: 435-48.

1299 Raze D, Verwaerde C, Deloison G *et al.* Heparin-Binding Hemagglutinin Adhesin (HBHA) Is Involved in
1300 Intracytosolic Lipid Inclusions Formation in Mycobacteria. *Front Microbiol* 2018;**9**: 2258.

1301 Reed MB, Gagneux S, Deriemer K *et al.* The W-Beijing lineage of Mycobacterium tuberculosis overproduces
1302 triglycerides and has the DosR dormancy regulon constitutively upregulated. *J Bacteriol* 2007;**189**:
1303 2583-9.

1304 Rodriguez GM, Voskuil MI, Gold B *et al.* *ideR*, An essential gene in mycobacterium tuberculosis: role of *IdeR*
1305 in iron-dependent gene expression, iron metabolism, and oxidative stress response. *Infect Immun*
1306 2002;**70**: 3371-81.

1307 Rodriguez JG, Hernandez AC, Helguera-Repetto C *et al.* Global adaptation to a lipid environment triggers the
1308 dormancy-related phenotype of Mycobacterium tuberculosis. *MBio* 2014;**5**: e01125-14.

1309 Russell DG. Mycobacterium tuberculosis: here today, and here tomorrow. *Nat Rev Mol Cell Biol* 2001;**2**: 569-
1310 77.

1311 Russell DG. Who puts the tubercle in tuberculosis? *Nat Rev Microbiol* 2007;**5**: 39-47.

1312 Russell DG, Cardona PJ, Kim MJ *et al.* Foamy macrophages and the progression of the human tuberculosis
1313 granuloma. *Nat Immunol* 2009;**10**: 943-8.

1314 Russell DG, VanderVen BC, Lee W *et al.* Mycobacterium tuberculosis wears what it eats. *Cell Host Microbe*
1315 2010;**8**: 68-76.

1316 Santucci P, Bouzid F, Smichi N *et al.* Experimental Models of Foamy Macrophages and Approaches for
1317 Dissecting the Mechanisms of Lipid Accumulation and Consumption during Dormancy and
1318 Reactivation of Tuberculosis. *Front Cell Infect Microbiol* 2016;**6**: 122.

1319 Santucci P, Diomande S, Poncin I *et al.* Delineating the Physiological Roles of the PE and Catalytic Domains of
1320 LipY in Lipid Consumption in Mycobacterium-Infected Foamy Macrophages. *Infection and immunity*
1321 2018;**86**.

1322 Santucci P, Johansen MD, Point V *et al.* Nitrogen deprivation induces triacylglycerol accumulation, drug
1323 tolerance and hypervirulence in mycobacteria. *Sci Rep* 2019a;**9**: 8667.

1324 Santucci P, Smichi N, Diomande S *et al.* Dissecting the membrane lipid binding properties and lipase activity
1325 of Mycobacterium tuberculosis LipY domains. *FEBS J* 2019b;**286**: 3164-81.

1326 Sassetti CM, Boyd DH, Rubin EJ. Genes required for mycobacterial growth defined by high density
1327 mutagenesis. *Mol Microbiol* 2003;**48**: 77-84.

1328 Schaefer WB, Lewis CW, Jr. Effect of oleic acid on growth and cell structure of mycobacteria. *J Bacteriol*
1329 1965;**90**: 1438-47.

1330 Schué M, Maurin D, Dhoub R *et al.* Two cutinase-like proteins secreted by *Mycobacterium tuberculosis* show
1331 very different lipolytic activities reflecting their physiological function. *Faseb J* 2010;**24**: 1893-903.

1332 Sheehan HL, Whitwell F. The staining of tubercle bacilli with Sudan black B. *J Pathol Bacteriol* 1949;**61**: 269-
1333 71, pl.

1334 Sherman DR, Voskuil M, Schnappinger D *et al.* Regulation of the Mycobacterium tuberculosis hypoxic
1335 response gene encoding alpha -crystallin. *Proc Natl Acad Sci U S A* 2001;**98**: 7534-9.

1336 Singh A, Crossman DK, Mai D *et al.* Mycobacterium tuberculosis WhiB3 maintains redox homeostasis by
1337 regulating virulence lipid anabolism to modulate macrophage response. *PLoS Pathog* 2009;**5**:
1338 e1000545.

1339 Singh KH, Jha B, Dwivedy A *et al.* Characterization of a secretory hydrolase from Mycobacterium tuberculosis
1340 sheds critical insight into host lipid utilization by M. tuberculosis. *J Biol Chem* 2017;**292**: 11326-35.

1341 Sirakova TD, Dubey VS, Deb C *et al.* Identification of a diacylglycerol acyltransferase gene involved in
1342 accumulation of triacylglycerol in Mycobacterium tuberculosis under stress. *Microbiology* 2006;**152**:
1343 2717-25.

1344 Timm J, Post FA, Bekker LG *et al.* Differential expression of iron-, carbon-, and oxygen-responsive
1345 mycobacterial genes in the lungs of chronically infected mice and tuberculosis patients. *Proc Natl
1346 Acad Sci U S A* 2003;**100**: 14321-6.

1347 Tong J, Liu Q, Wu J *et al.* Mycobacterium tuberculosis strains of the modern Beijing sublineage excessively
1348 accumulate triacylglycerols in vitro. *Tuberculosis (Edinb)* 2020;**120**: 101892.

1349 Uzbekov R, Roingard P. Nuclear lipid droplets identified by electron microscopy of serial sections. *BMC Res
1350 Notes* 2013;**6**: 386.

1351 Via LE, Lin PL, Ray SM *et al.* Tuberculous granulomas are hypoxic in guinea pigs, rabbits, and nonhuman
1352 primates. *Infection and immunity* 2008;**76**: 2333-40.

1353 Vijay S, Hai HT, Thu DDA *et al.* Ultrastructural Analysis of Cell Envelope and Accumulation of Lipid Inclusions
1354 in Clinical Mycobacterium tuberculosis Isolates from Sputum, Oxidative Stress, and Iron Deficiency.
1355 *Front Microbiol* 2017;**8**: 2681.

1356 Vilcheze C, Kremer L. Acid-Fast Positive and Acid-Fast Negative Mycobacterium tuberculosis: The Koch
1357 Paradox. *Microbiol Spectr* 2017;**5**.

1358 Vilcheze C, Molle V, Carrere-Kremer S *et al.* Phosphorylation of KasB regulates virulence and acid-fastness in
1359 Mycobacterium tuberculosis. *PLoS pathogens* 2014;**10**: e1004115.

1360 Viljoen A, Blaise M, de Chastellier C *et al.* MAB_3551c encodes the primary triacylglycerol synthase involved
1361 in lipid accumulation in Mycobacterium abscessus. *Molecular microbiology* 2016, DOI
1362 10.1111/mmi.13482.

1363 Voskuil MI, Schnappinger D, Visconti KC *et al.* Inhibition of respiration by nitric oxide induces a
1364 Mycobacterium tuberculosis dormancy program. *J Exp Med* 2003;**198**: 705-13.

1365 Waltermann M, Hinz A, Robenek H *et al.* Mechanism of lipid-body formation in prokaryotes: how bacteria
1366 fatten up. *Mol Microbiol* 2005;**55**: 750-63.

1367 Wältermann M, Steinbüchel A. Neutral lipid bodies in prokaryotes: recent insights into structure, formation,
1368 and relationship to eukaryotic lipid depots. *J Bacteriol* 2005;**187**: 3607-19.

1369 Walther TC, Farese RV, Jr. The life of lipid droplets. *Biochim Biophys Acta* 2009;**1791**: 459-66.

1370 Wayne LG, Sohaskey CD. Nonreplicating persistence of mycobacterium tuberculosis. *Annu Rev Microbiol*
1371 2001;**55**: 139-63.

1372 Weir MP, Langridge WH, 3rd, Walker RW. Relationships between oleic acid uptake and lipid metabolism in
1373 Mycobacterium smegmatis. *Am Rev Respir Dis* 1972;**106**: 450-7.

1374 WHO. Global tuberculosis Report.
1375 <https://apps.who.int/iris/bitstream/handle/10665/336069/9789240013131-eng.pdf> 2020.

1376 Williams KJ, Jenkins VA, Barton GR *et al.* Deciphering the metabolic response of Mycobacterium tuberculosis
1377 to nitrogen stress. *Mol Microbiol* 2015;**97**: 1142-57.

1378 Zhang C, Yang L, Ding Y *et al.* Bacterial lipid droplets bind to DNA via an intermediary protein that enhances
1379 survival under stress. *Nat Commun* 2017;**8**: 15979.

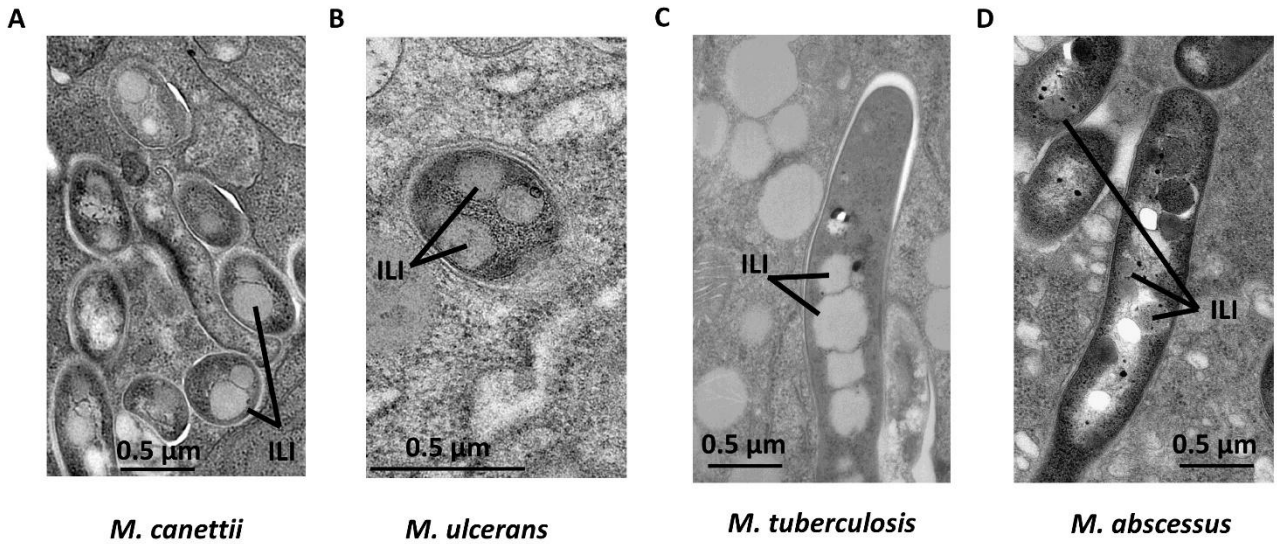
1380

1381

1382 **Figures and Figure legends**

1383

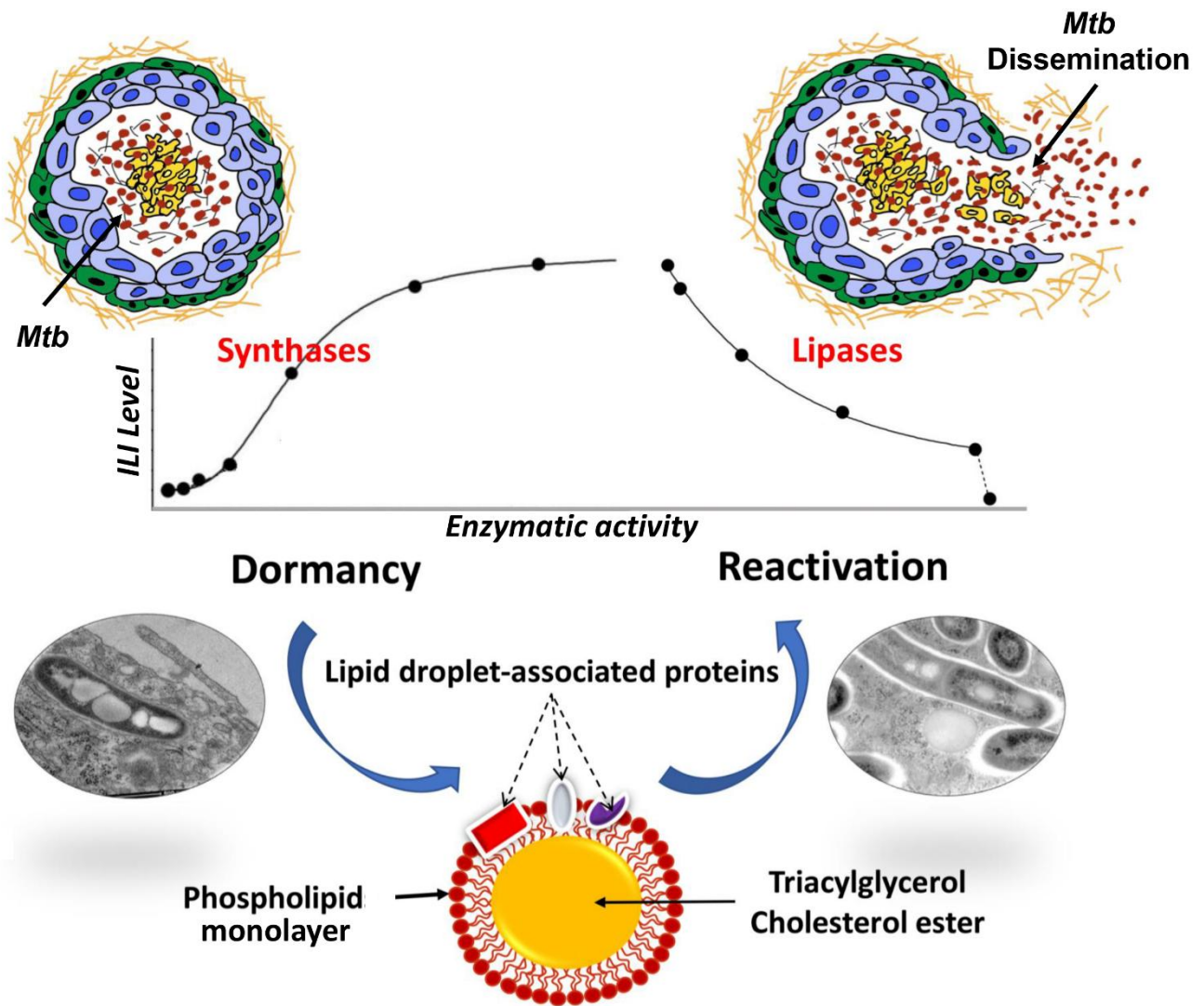
1384



1385

1386

1387 **Figure 1:** Electron microscopy images of ILI in various intracellular pathogenic
1388 mycobacteria inside different hosts. **(A)** 3T3-L1 mature adipocytes infected with *M. canettii*.
1389 **(B)** Mouse tail tissue infected with *M. ulcerans*. **(C)** *Mtb*-infected cell from a sputum sample
1390 from a TB-positive patient. **(D)** *M. abscessus*-containing macrophage in a zebrafish embryo.
1391 ILI are indicated with black lines and scale bars represent 0.5 μm. All electron microscopy
1392 micrographs depicted are from the authors' personal collections.
1393

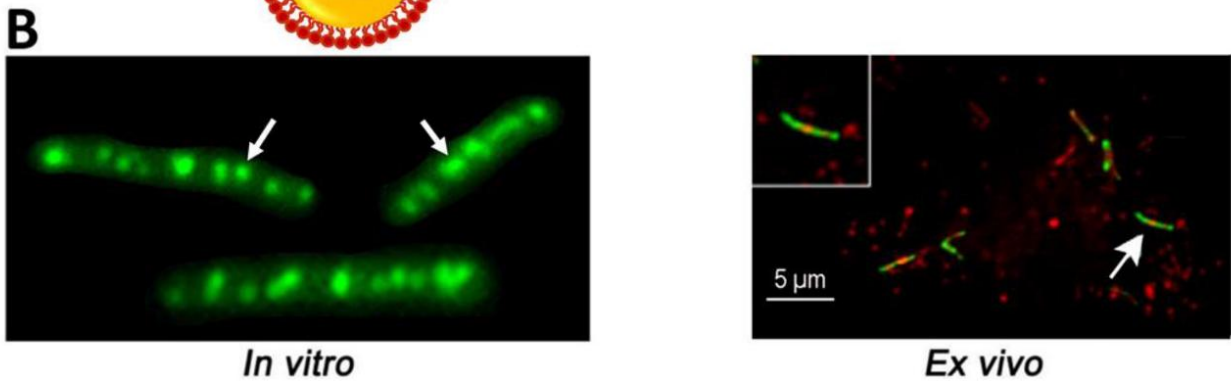
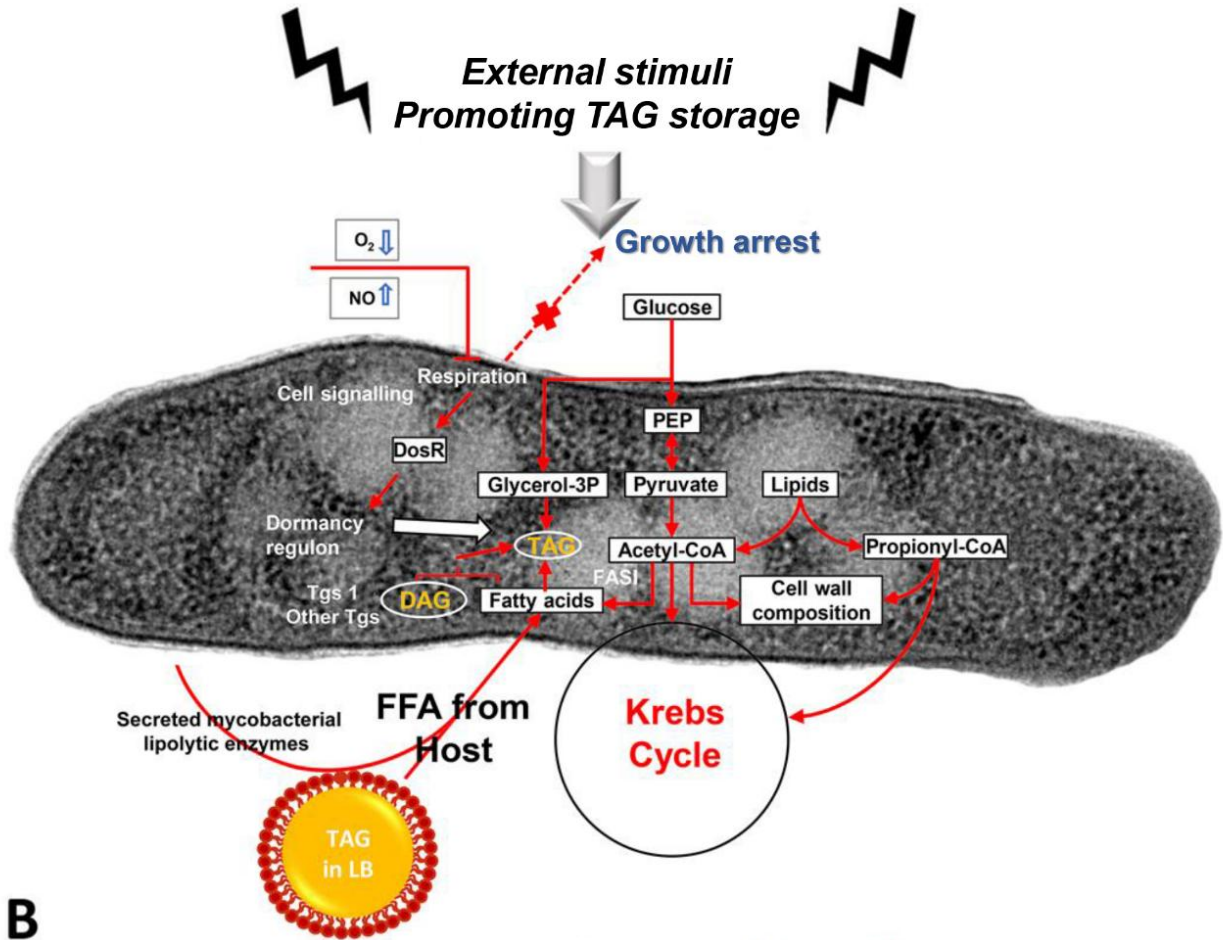


1394
 1395
 1396
 1397
 1398
 1399
 1400
 1401

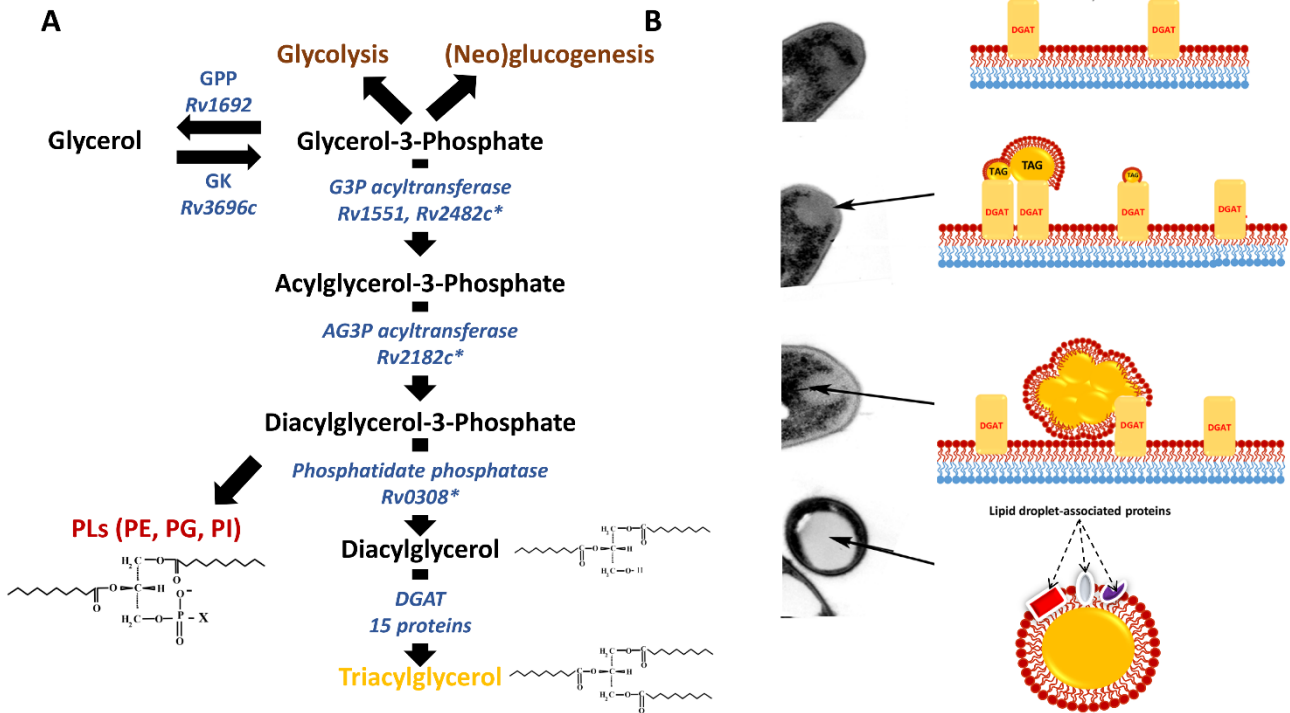
Figure 2: Scheme showing the role of synthases during ILI formation stage and the engagement of lipases during the ILI consumption stage, which are related to dormancy and reactivation, respectively. As observed in the electron microscopy picture on the right, total ILI consumption is not required for regrowth/reactivation/transmission. All electron and confocal microscopy pictures were from the authors' personal collections.

A Environment Infection

Osmolarity, Temperature, Altered pH, Hypoxia, Iron/zinc/nitrogen limitation, ROS/PNS



1402
 1403 **Figure 3:** Different stimuli promoting ILI formation in mycobacteria are indicated by black
 1404 arrows. **(A)** The metabolic pathway inducing TAG synthesis and their accumulation to form
 1405 ILI is indicated inside bacteria. From the literature host FFA providing from TAG contained
 1406 in LD are mainly due to the action of secreted mycobacterial lipolytic enzymes (Santucci, et
 1407 al. 2018), **(B)** Confocal microscopic imaging of mycobacteria under ILI-promoting conditions
 1408 using *in vitro* (left panel) and *ex vivo* (right panel) models. For the latter, BMDM were
 1409 infected with the GFP-expressing *Mbv* BCG strain. Six days later, cells were exposed to
 1410 VLDL for 24 hr. Cells were then treated with BODIPY (red label), which stains neutral lipids
 1411 prior fixation and observation under the confocal microscope. After a 24 hr exposure to
 1412 VLDL, both the macrophage and *Mbv* BCG (arrow and insert) contained BODIPY-stained
 1413 granules (orange). All electron and confocal microscopy pictures were from the authors'
 1414 personal collections.



1415

1416

1417

1418

1419

1420

1421

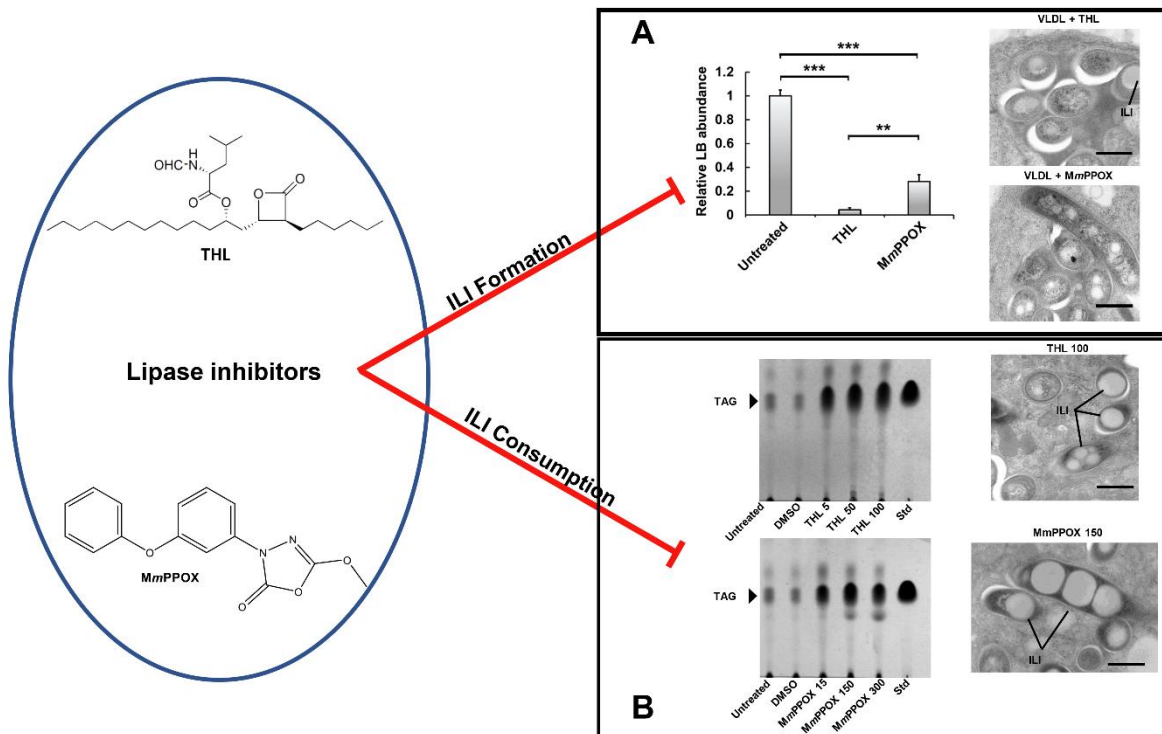
1422

1423

1424

1425

Figure 4: Synthesis of TAG into Actinobacteria. **(A)** Enzymes and substrates involved in TAG synthesis (Kennedy pathway), homolog in *M. tuberculosis* are indicated. **(B)** Scheme of lipid droplet formation based on the electron microscopy observation in *R. opacus* PD630 (adapted from (Wältermann and Steinbüchel 2005)). GPP: glycerol phosphate phosphatase (*Rv1692* (Larrouy-Maumus, et al. 2013)), GK: Glycerol kinase (*Rv3696c* (Maarsingh and Haydel 2018)), GPAT: Glycerol 3 Phosphate acyltransferase (*Rv1551* (Law and Daniel 2017), *Rv2482c**), PAP, Phosphatidate phosphatase (*Rv0308**), DGAT: Diacylglycerol acetyl transferase, PL: Phospholipids, X: Ethanolamine or Choline or Inositol, TAG Triacylglycerol. Star means putative.



1426

1427 **Figure 5:** Pharmacological inhibition targeting lipolytic enzymes modulates ILI formation
 1428 and consumption. Chemical structures of lipases inhibitors THL and MmPPOX are
 1429 displayed on the left panel. On the right panel, a schematic representation displays their
 1430 effects onto **(A)** ILI formation through enzymatic inhibition of host-cell proteins involved in
 1431 LD biogenesis within the VLDL-induced FM model (Adapted from (Santucci, et al. 2018))
 1432 and **(B)** ILI breakdown *in vitro* and during macrophages infection. Electron micrographs and
 1433 thin layer chromatography (adapted from (Santucci, et al. 2019a)) show the absence of
 1434 TAG degradation in presence of THL or MmPPOX compounds. Scale bars represent 0.5
 1435 μm .

1436

1437

1438

1439